Bacterial inoculation elicits changes to the coral epigenome

Adam R. Barno[1], Helena D.M. Villela[1], Pedro M. Cardoso[1], Francisca C. García[1], Guoxin Cui[1], Nathalia Delgadillo-Ordoñez[1], Alexandre S. Rosado[1], Torsten Thomas[2], Manuel Aranda[1], Christian R. Voolstra[3], Raquel S. Peixoto *[1]

[1] Biological and Environmental Science and Engineering Division (BESE), King Abdullah University of Science and Technology, Thuwal, Makkah, Kingdom of Saudi Arabia

[2] Centre for Marine Science and Innovation, School of Biological, Earth and Environmental Sciences, University of New South Wales, Australia

[3] Department of Biology, University of Konstanz, Konstanz, Germany

* Correspondence: Raquel S. Peixoto, raquel.peixoto@kaust.edu.sa

Keywords: climate change, pathogens, coral probiotics, Beneficial Microorganisms for Corals (BMCs), microbiome manipulation, DNA methylation

Abstract

Environmental shifts can cause epigenetic modifications in corals, which are associated with changes in gene expression and physiology, though it remains unclear if associated bacteria can also induce such changes. Here, we inoculated nubbins of the coral *Pocillopora verrucosa* with an opportunistic pathogen, *Vibrio coralliilyticus*, and/or a coral probiotic, *Cobetia* sp., and subjected the nubbins to heat stress. We show that pathogen exposure led to distinct DNA methylation changes compared to the control, probiotic, and co-inoculation groups. We also demonstrate that DNA methylation correlates with coral gene expression and highlight genes altered by pathogen inoculation that showed similar responses in their expression and methylation. Notably, the coral probiotic was able to mitigate specific epigenetic changes, which correlated with increased stress resilience and higher coral survival rates. Thus, bacterial-induced changes to the coral epigenome may instigate long-term changes in host resilience.

38 **Main**

39

40 Recent work has shown that beneficial bacteria (probiotics) can increase coral health and
41 resilience in response to stress caused by pathogens, increased temperature, and oil
42 spills[1-7]. This is because bacteria are essential to the proper functioning of the coral
43 holobiont[8-10], which consists of the coral animal and its associated symbiotic microbes.
44 For example, inoculation of the coral *Pocillopora damicornis* with beneficial
45 microorganisms for corals (BMCs) consisting of bacteria from the genera *Yangia*,
46 *Roseobacter*, *Phytobacter*, and *Salinicola*, correlated with increases in energy reserves
47 and calcification rates[11]. Furthermore, administration of BMCs during and after heat
48 stress increased transcription of genes involved in recovery and stress attenuation and
49 decreased those related to inflammatory and innate immune responses in the coral
50 *Mussismilia hispida*[5]. These changes also correlated with improved coral survival and
51 increased photosynthetic efficiency in the associated symbiotic microalgae (i.e.,
52 Symbiodiniaceae)[5]. High temperatures, though, can also lead to dysbiosis and increased
53 establishment of opportunistic pathogens, causing coral bleaching and death[5,12]. For
54 example, inoculation with the temperature-dependent coral pathogen *Vibrio*
55 *coralliilyticus* brought about a reduction in the skeletal density and abnormal crystal
56 morphology in *P. damicornis*[3]. This could be attenuated by inoculation with a BMC
57 consortium composed of bacteria from the genera *Pseudoalteromonas*, *Cobetia*, and
58 *Halomonas*[3], showing the protective capacity of BMCs against pathogens as well as
59 temperature stress.

60

61 Coral-associated microorganisms have recently been posited to have the ability to alter
62 coral epigenomes, thus modifying phenotypic responses[13]. The most commonly studied
63 epigenome modification in corals is DNA methylation, which, depending on the location
64 of the methylated bases, prevents transcriptional noise and increases fidelity[14-16]. The
65 interaction between coral epigenomes and their symbionts was recently demonstrated by
66 exchanging the Symbiodiniaceae strain in the coral *Montastraea cavernosa* and applying
67 thermal stress, which together produced changes in DNA methylation[17]. Exchanging or
68 manipulating bacterial symbionts may have similar impacts on the coral host, however
69 this has not been studied. These impacts could be either indirect, by changing the
70 nutritional status or altering metabolic capacities[10], or direct, by producing metabolites
71 that act as cofactors for epigenome-modifying enzymes[18] or encoding proteins that are
72 homologs of bacteria-produced proteins capable of inducing epigenomic changes in
73 mammals[13].
74
75 Here, we sought to determine whether inoculation with bacteria leads to changes in the
76 coral epigenome that align with improved resilience to thermal stress. To do this, we
77 regularly inoculated *P. verrucosa* nubbins with either a BMC (*Cobetia* sp. strain
78 pBMC4[19]; hereafter "*Cobetia*"), a temperature-dependent pathogen (*V. coralliilyticus*
79 strain BAA-450[20]; hereafter "*Vibrio*"), or both bacteria (hereafter "Both"), and subjected
80 the corals to a temperature stress regime (from 27 ˚C to 33 ˚C), followed by a recovery
81 period. Heat-stressed corals are hereafter denoted with "H_", whereas corals kept at
82 ambient temperature throughout the experiment are denoted with "A_". The mesocosm
83 experiment encompassed 28 days, with samples taken before any inoculation was applied

84 (T0 = day 0), at the peak of the heat stress (T1 = day 19), and after a recovery period (T2
85 = day 28). DNA methylation differences at the gene level were analyzed and linked to
86 increases in the abundance of the respective inocula, gene expression levels, and coral
87 phenotypic responses, to show that bacterial inoculation, in combination with temperature
88 stress, can modulate the coral epigenome. Through co-inoculation of a probiotic and
89 pathogen, we could further show that indicators of stress seen in the pathogen-inoculated
90 corals were reduced with the co-inoculated BMC. This pattern could be observed in all
91 components of the holobiont (host phenotype, host epigenome, host gene expression,
92 symbiont photosynthetic efficiency, and microbiome composition) and underscores the
93 potential for probiotic therapy as prevention of epigenomic disturbances caused by
94 pathogenic infection.
95
96 **Results**
97
98 *Probiotic inoculation increases coral resilience*
99
100 To evaluate the effects of bacterial inoculation and temperature stress on *P. verrucosa*,
101 we monitored nubbin health over a 28-day mesocosm experiment using photosynthetic
102 efficiency measurements and nubbin condition/coloration. This showed that *Vibrio*
103 inoculation negatively affected coral resilience to temperature stress during recovery,
104 while the *Cobetia* and co-inoculation groups showed more resilience. The photosynthetic
105 efficiency (*Fv*/*Fm* values measured by Diving-PAM II) was significantly lower in heat-
106 stressed corals than in ambient temperature corals at T1 (*Wilcoxon Rank Sum*: $W = 256$, p
107 = 1.54e-6) and T2 (*Wilcoxon Rank Sum*: $W = 248$, p = 6.64e-6) (Fig. 1A and

Supplementary Table 1a). The *Fv/Fm* values were not significantly different between inoculation groups in either the ambient temperature corals (*Kruskal-Wallis*: $X^2 = 4.87$, df = 3, p = 0.182) nor the heat-stressed corals (*Kruskal-Wallis*: $X^2 = 3.97$, df = 3, p = 0.265) at T2, although the mean *Fv/Fm* for H_*Vibrio* was lower than the other heat-stressed groups (0.368 ± 0.245 for H_*Vibrio*, 0.523 ± 0.047 for H_Control, 0.514 ± 0.045 for H_*Cobetia*, 0.530 ± 0.012 for H_Both).

Color intensity of coral tissue was measured by converting each image to grayscale and calculating the average intensity (from 0 = black, to 256 = white) across the whole image of the coral nubbin. Thus, a lower average color intensity would represent darker, i.e., healthier, living tissue, and a higher color intensity would represent pale, bleached, or dead coral tissue. Similar to previous findings[4], the combination of heat stress and *Vibrio* inoculation (H_*Vibrio*) resulted in significantly higher color intensity, i.e., 'whiteness' or paling, (*Kruskal-Wallis*: $X^2 = 8.49$, df = 3, p = 0.037; *Dunn test*: p = 0.043; Fig. 1B) and lower percentage live tissue (*Kruskal-Wallis*: $X^2 = 10.08$, df = 3, p = 0.018; *Dunn test*: p = 0.014; Fig. 1C) when compared to the control group (H_Control) after the recovery period (T2) (Supplementary Table 1b). Notably, both the color intensity and percentage of live tissue in all other inoculation groups within the same temperature regime, including the co-inoculation group, were statistically indistinguishable from each other (Fig. 1B-C). Although the *Vibrio*-inoculated coral nubbins were paler than the nubbins from the other experimental groups at T2 in the heat-stressed corals, the color intensities of the live tissue remaining on the coral nubbins were not significantly different (*Kruskal-Wallis*: $X^2 = 7.48$, df = 3, p = 0.058; Extended Data Fig. 1).

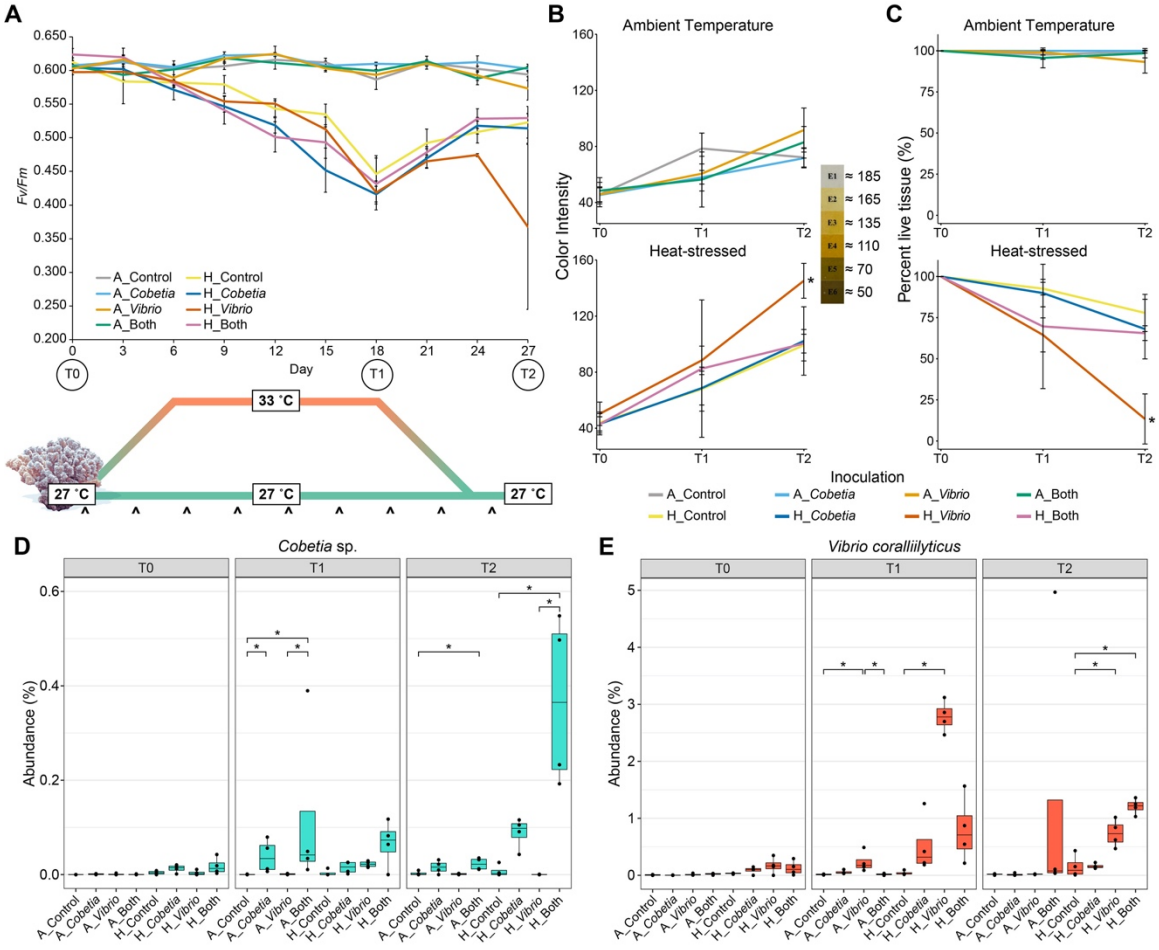

Fig. 1. Coral phenotypic response and inoculated bacteria abundances throughout the experiment. (A) Mean photosynthetic efficiency (*Fv/Fm* ratios; y axis) from coral nubbins during the mesocosm experiment days (x axis). The error bars represent standard deviations (n = 4). Carets (^) below the schematic represent days of bacteria inoculation (every 3 days starting from day 1). (B) Average color intensity and (C) percentage live tissue of the coral nubbins in each condition, as measured by ImageJ (T0: n = 12 per group; T1/T2: n = 4 per group). Lines represent the mean value for each condition, and the error bars represent standard deviations. Higher color intensities represent more paling, bleaching, or tissue loss. Color intensity was measured on the CoralWatch Coral Health Chart[21] for reference. Percentage abundances are shown in boxplots of the bacterial inocula (*Cobetia* sp. (D) and *V. coralliilyticus* (E)) across inoculations and sampling times (n = 4 per group). Boxplots display the individual data points, medians, lower and upper quartiles, and whiskers displaying the 1.5x interquartile range. Abundances of each inoculum were compared between each inoculation group (i.e., Control, *Cobetia*, *Vibrio*, Both) within each temperature condition (i.e., ambient temperature or heat-stressed). Asterisks denote significant differences between groups within a timepoint (*Dunn test*: $p < 0.05$).

149 Using 16S rRNA gene analysis, we found that the relative abundance of *V. coralliilyticus*
150 was significantly higher in the corals treated with the pathogen than the control group at
151 T1 (*Kruskal-Wallis*: X^2 = 13.059, df = 3, p = 0.005; *Dunn test*: p = 0.002) and T2
152 (*Kruskal-Wallis*: X^2 = 11.647, df = 3, p = 0.009; *Dunn test*: p = 0.045) (Fig. 1D-E and
153 Supplementary Table 2). The abundance of *Vibrio* in the co-inoculation groups were
154 lower than the *Vibrio*-inoculations at T1, but not at T2, although these differences were
155 only significant between A_*Vibrio* and A_Both at T1 (*Kruskal-Wallis*: X^2 = 11.978, df =
156 3, p = 0.007; *Dunn test*: p = 0.023). This coincided with increased microbiome alpha
157 diversity in all heat-stressed groups at T2 (Extended Data Fig. 2) and microbiome
158 restructuring in the heat-stressed groups at T1 and T2 marked by a decrease in members
159 of the family Endozoicomonadaceae, and increases in Saprospiraceae and
160 Rhodobacteraceae (Extended Data Fig. 3). Significant differences in beta diversity were
161 also observed between temperature groups and between the bacterial inoculation groups
162 within both temperature conditions at T1 and T2 (Extended Data Fig. 4, Supplementary
163 Table 3a and 3b).
164
165 *Coral epigenomes respond to temperature stress and bacterial inoculation*
166
167 To explore whether the stress mitigation in co-inoculated coral nubbins was also
168 attributed to interactions with the coral epigenome, genome-wide differences in DNA
169 methylation were analyzed in response to temperature stress, bacterial inoculation, and
170 their interaction. The profile of median methylation levels of genes across the genome of
171 *P. verrucosa* were visualized with a non-metric multidimensional scaling (nMDS) plot
172 for each timepoint (Fig. 2, Supplementary Table 4a). Significant differences existed at the

173 peak of stress (T1) between corals exposed to the heat stress and those that were not
174 (*PERMANOVA*: R^2 = 0.107, F = 3.245, p = 0.001; *PERMDISP*: p = 0.981), showing that
175 methylation marks can change after twelve days of constant exposure to temperature
176 stress (and 19 days of experimentation).
177
178 The difference between samples subjected to different temperature conditions was also
179 observed after 9 days of recovery (28 days total; T2) (*PERMANOVA*: R^2 = 0.061, F =
180 1.955, p = 0.002; *PERMDISP*: p = 0.399). Additionally, 'time' was a significant factor in
181 separating the heat-stressed corals using genome-wide DNA methylation levels, and
182 pairwise comparisons showed significant differences between each of the timepoint pairs
183 T0-T1, T1-T2, and T0-T2 (Extended Data Fig. 5). Bacterial inoculation groups also
184 significantly contributed to the separation of samples at T2 (*PERMANOVA*: R^2 = 0.112, F
185 = 1.197, p = 0.028; *PERMDISP*: p = 0.412), but there was not statistical support for the
186 interaction between temperature and bacteria inoculations (*PERMANOVA*: R^2 = 0.106, F
187 = 1.133, p = 0.106). Pairwise comparisons showed that pathogen-inoculated corals were
188 significantly different from the control corals (*PERMANOVA*: R^2 = 0.101, F = 1.456, p =
189 0.029), but there was no statistical support for pairwise differences between any of the
190 other inoculation groups at T2 (Supplementary Table 4b).
191

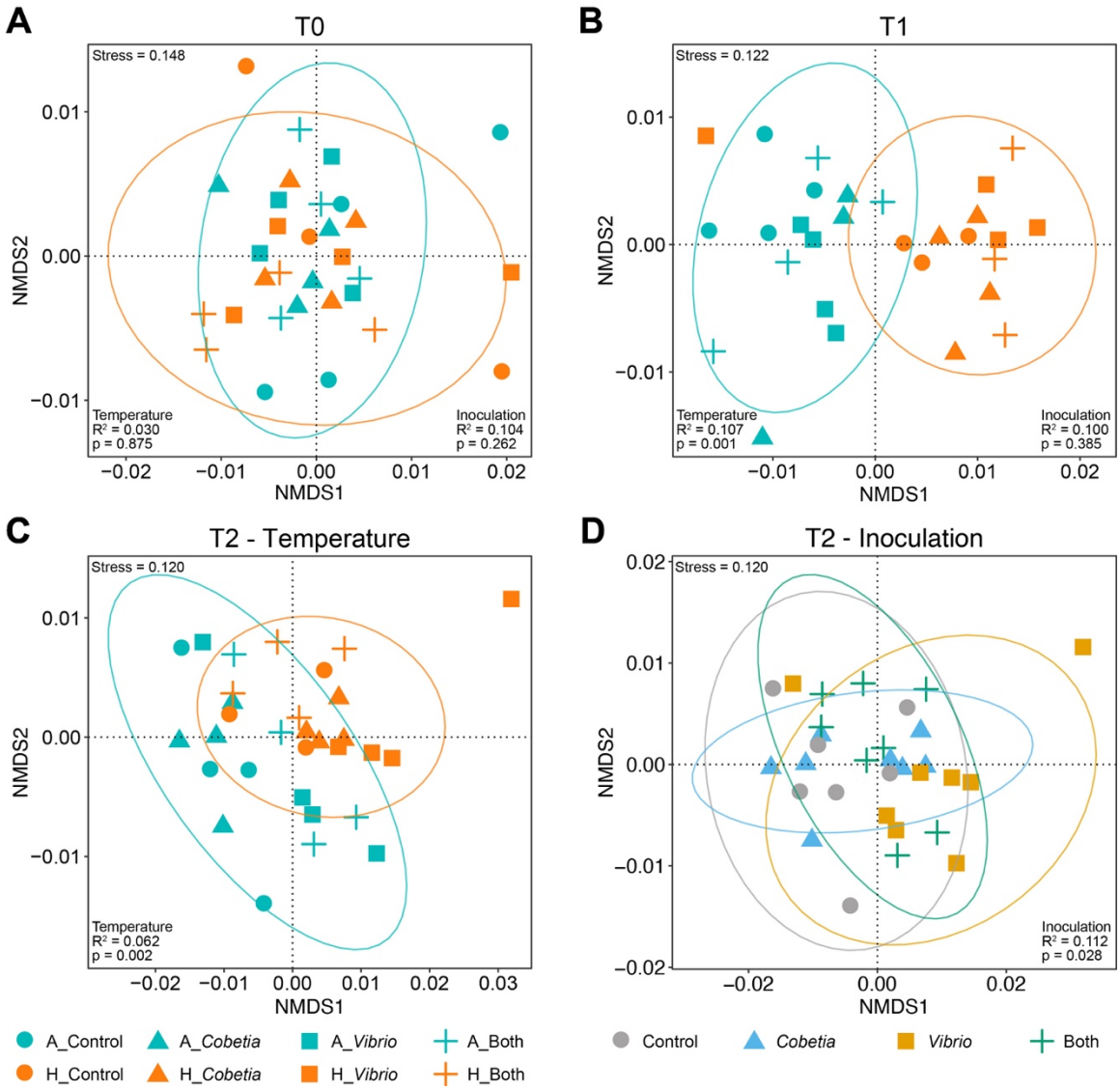

Fig. 2. Non-metric MultiDimensional Scaling (nMDS) plots based on Bray-Curtis dissimilarities of the median methylation levels of genes across the genome of *P. verrucosa*. Samples from each timepoint were separated using Bray-Curtis dissimilarity and plotted along the first two dimensions. Circles = 95% confidence intervals around temperature groups. Both temperature and inoculation were tested as factors driving the separation between groups using PERMANOVA at (A) T0, (B) T1, and T2. R^2 and p-values are displayed, representing the magnitude and significance attributed to each of the factors (n = 4 per group, except A_Control at T1, H_Control at T0,/T1/ T2, and H_Both at T1, where n = 3). nMDS plots for T2 are shown highlighting differences based on (C) temperature and (D) bacteria inoculation.

Pathogen inoculation leads to changes in gene methylation

205

206 The significant genome-wide differences in median methylation levels observed between
207 the temperature conditions at T1 and the temperature conditions and bacteria inoculation
208 groups at T2 (Fig. 2) were further investigated using pairwise generalized linear models
209 (GLMs). A total of 932 genes were significantly associated with temperature differences
210 at T1, and 313 genes were significantly associated with the different temperature groups
211 at T2 (Extended Data Fig. 6, Supplementary Table 5a and 5b). At T2, 17 genes were
212 found to be significantly influenced by *Vibrio* inoculation in comparison to the control
213 group, 15 of which had depleted median methylation levels correlated with *Vibrio*
214 inoculation (Supplementary Table 5c). Extending the comparison of these 17 genes to the
215 other inoculation groups using hierarchical clustering based on Euclidean distances
216 shows that coral nubbins inoculated with *Vibrio* separated from the other three conditions
217 at T2 (Fig. 3). These results corroborate the stressed physiological response of the coral
218 nubbins caused by *Vibrio* inoculation observed at T2 (Fig. 1B-C) because it shows that
219 the other inoculation groups (*Cobetia* and Both) cluster more closely to the Control group
220 than the *Vibrio* inoculation in these genes. This demonstrates that, although pathogen
221 inoculation significantly alters coral DNA methylation, co-inoculation of the pathogen
222 and BMC leads to methylation patterns similar to the control group, supporting the notion
223 that BMCs negate impacts caused by pathogen stress on coral health.
224

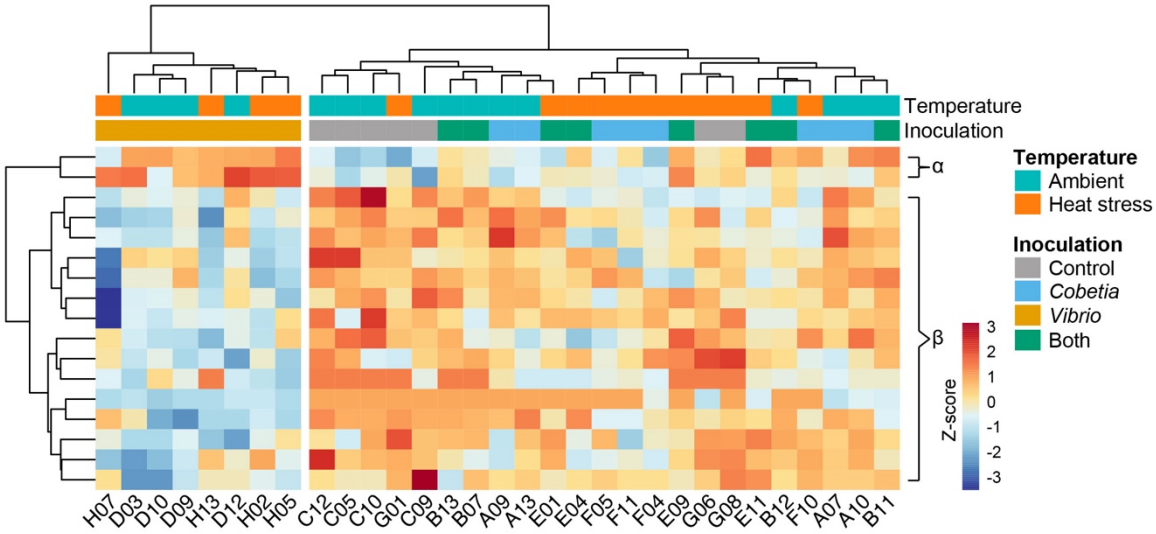

GO:ID	Enriched biological process found in cluster β
GO:0072673	lamellipodium morphogenesis
GO:0034498	early endosome to Golgi transport
GO:0035871	protein K11-linked deubiquitination
GO:0035627	ceramide transport
GO:0035520	monoubiquitinated protein deubiquitination
GO:0007196	adenylate cyclase-inhibiting G protein-coupled glutamate receptor signaling pathway
GO:0070212	protein poly-ADP-ribosylation
GO:0007097	nuclear migration
GO:0002181	cytoplasmic translation
GO:0036297	interstrand cross-link repair
GO:0008053	mitochondrial fusion
GO:0006282	regulation of DNA repair
GO:0035082	axoneme assembly
GO:0051966	regulation of synaptic transmission, glutamatergic

Fig. 3. Genes with median methylation levels significantly associated with *Vibrio* inoculation according to GLMs compared to samples from other inoculation groups at T2 (n = 4; n = 3 for H_Control). There is a separation between the corals inoculated with *V. coralliilyticus* and the other inoculation groups (x-axis). Hierarchical clustering was performed using Euclidean distances and the "ward.D2" agglomeration method. The heights of the dendrograms, representing distances separating the clusters, ranged from 2.6 to 18.3 between the coral samples and 4.0 and 14.1 between the methylated genes. Colors represent the z-score for any given gene. The enriched GO terms using TopGO display the significant functions with depleted methylation levels in pathogen-stressed corals (cluster β). All enriched GO terms are in Supplementary Table 6c. All GO terms associated with these genes are in Supplementary Table 7.

Increases in gene body methylation reduce spurious transcription in highly expressed genes, thereby reinforcing the epigenetic control of genes as expression increases[14-16]. Our findings here revealed that methylation within *P. verrucosa* occurred primarily within the gene body (Extended Data Fig. 7, Supplementary Table 8). Genes with

241 depleted methylation in the corals treated with *Vibrio* only (cluster β in Fig. 3) highlight
242 the link between pathogen stress and diminished epigenetic control of genes involved in
243 cell maintenance and functioning and genes related to the immune system, which
244 potentially correlates with decreased gene expression.
245
246 The enriched GO terms in cluster β included "adenylate cyclase-inhibiting G protein-
247 coupled glutamate receptor signaling pathway" and the "regulation of synaptic
248 transmission (glutamatergic)", which both rely on the neurotransmitter glutamate.
249 Glutamate production is necessary for algal symbiosis in the cnidarian model *Aiptasia*[22].
250 Moreover, in the coral *Stylophora pistillata*, heat stress was found to disrupt glutamate
251 biosynthesis and trigger glutamate catabolism, which contributed to coral bleaching[23].
252 Therefore, pathogen inoculation may exacerbate losses in glutamate caused by heat stress
253 by reducing the epigenetic control of glutamatergic signal transduction. This may be
254 further supported by significant differences at T2 in the GO term "glutamatergic synapse"
255 (GO:0098978) due to temperature conditions (Supplementary Table 6b), although
256 additional research in this area is necessary, as heat stress did not induce uniform
257 methylation trends in all of the affected glutamatergic synapse genes (Extended Data Fig.
258 8). Further coral immune functions with depleted median methylation levels due to
259 *Vibrio* inoculation include "lamellipodium morphogenesis", "early endosome to Golgi
260 transport", and the stress response mechanisms "interstrand cross-link repair" and
261 "regulation of DNA repair".
262
263 *Pathogen inoculation affects gene expression*

264

265 To determine whether the methylation changes correlated with changes in gene
266 expression levels, the transcriptomes of the T2 nubbins were analyzed using RNA-Seq.
267 Heat stress and pathogen inoculation caused distinct transcriptome changes, with
268 H_*Vibrio* samples separating from the other groups in a principal component analysis
269 (PCA) plot along PC1 (which accounted for 74.93% of the variance) (Fig. 4A).
270 Hierarchical clustering also showed that three of the four H_*Vibrio* samples separated
271 distinctly from the other groups (Fig. 4B). The median methylation levels across the
272 genome positively correlated with the relative expression level of genes ($R^2 = 0.084$, $p <$
273 2e-16; Fig. 4C). Of the 17 genes with altered methylation due to pathogen inoculation,
274 four showed a significant correlation between changes in methylation and gene
275 expression across experimental groups (Fig 4D and Supplementary Table 9). Three of the
276 genes: g13505, g16333, and g8986, were positively correlated with gene methylation,
277 and were defined by the GO terms related to transmembrane transporter activity, negative
278 regulation of transcription by RNA polymerase II, and cilium movement, respectively
279 (Supplementary Table 7). One gene, g1533, was negatively correlated with gene
280 methylation and was not associated with a GO term (Supplementary Table 7).
281

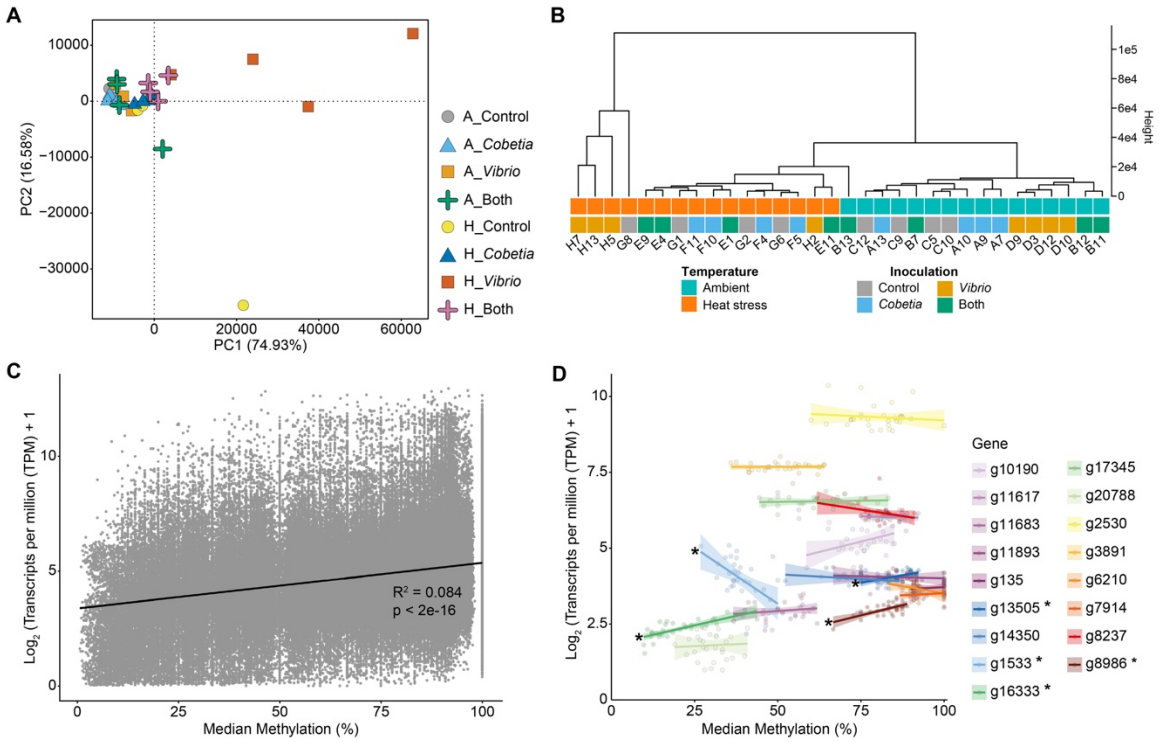

Fig 4. Gene expression levels are affected by heat stress and bacteria inoculation and correlated with methylation levels at T2. (A) PCA generated from the transcripts per million (TPM) expression estimates of *P. verrucosa* genes (n = 4). (B) Hierarchical clustering using the "ward.D2" agglomeration method to separate TPM values across the samples (n = 4). (C) A linear model shows that median methylation levels for all of the genes across all 31 samples were significantly and positively correlated with gene expression (using Log_2 (TPM + 1). The R^2 and p-value here represents the magnitude and significance attributed to the correlation. (D) The 17 genes with median methylation percent affected by pathogen inoculation are plotted against their respective gene expression. Four of these genes had median methylation levels, which significantly correlated with gene expression (denoted with asterisks).

Gene methylation differences are correlated with phenotypic response

To determine which genes affected by *Vibrio* inoculation (Fig. 3) correlated most with the paling and tissue loss observed in the corals (Fig. 1), linear models were implemented using the median methylation levels and color intensity as factors (Supplementary Table 10). The genes showing the highest correlation between methylation percentage and phenotypic response ($R^2 > 0.100$ and $p < 0.05$) were g16333, g1533, g17345, g14350,

301 and g8986 (Fig. 5). Example GO terms describing these genes were “negative regulation
302 of transcription by RNA polymerase II” (GO:0000122), N/A, “ceramide transport”
303 (GO:0035627), “adenylate cyclase-inhibiting G protein-coupled glutamate receptor
304 signaling pathway” (GO:0007196), and “cilium movement” (GO:0003341), respectively
305 (Supplementary Table 7). Of the genes with defined functions, three are related to
306 cellular processes, while g17345 (“ceramide transport”) functions in macromolecule
307 localization within the cell. In all of the defined genes, *Vibrio*-inoculation led to a
308 significant depletion in DNA methylation when compared to the control group in either
309 the ambient temperature or heat-stressed conditions. In all but one gene (g16333), co-
310 inoculation with *Cobetia* prevented similar decreases in DNA methylation when
311 compared with the control group. The genes g14350, defined by the GO term “adenylate
312 cyclase-inhibiting G protein-coupled glutamate receptor signaling pathway”, and g1533,
313 had significantly different median methylation levels between *Vibrio*-treated corals and
314 the co-inoculation in the heat-stressed condition (*ANOVA*: $F = 4.46$, df = 3, $p = 0.028$,
315 *TukeyHSD*: $p = 0.033$ for g14350; *ANOVA*: $F = 11.62$, df = 3, $p = 0.001$, *TukeyHSD*: $p =$
316 0.014 for g1533).
317

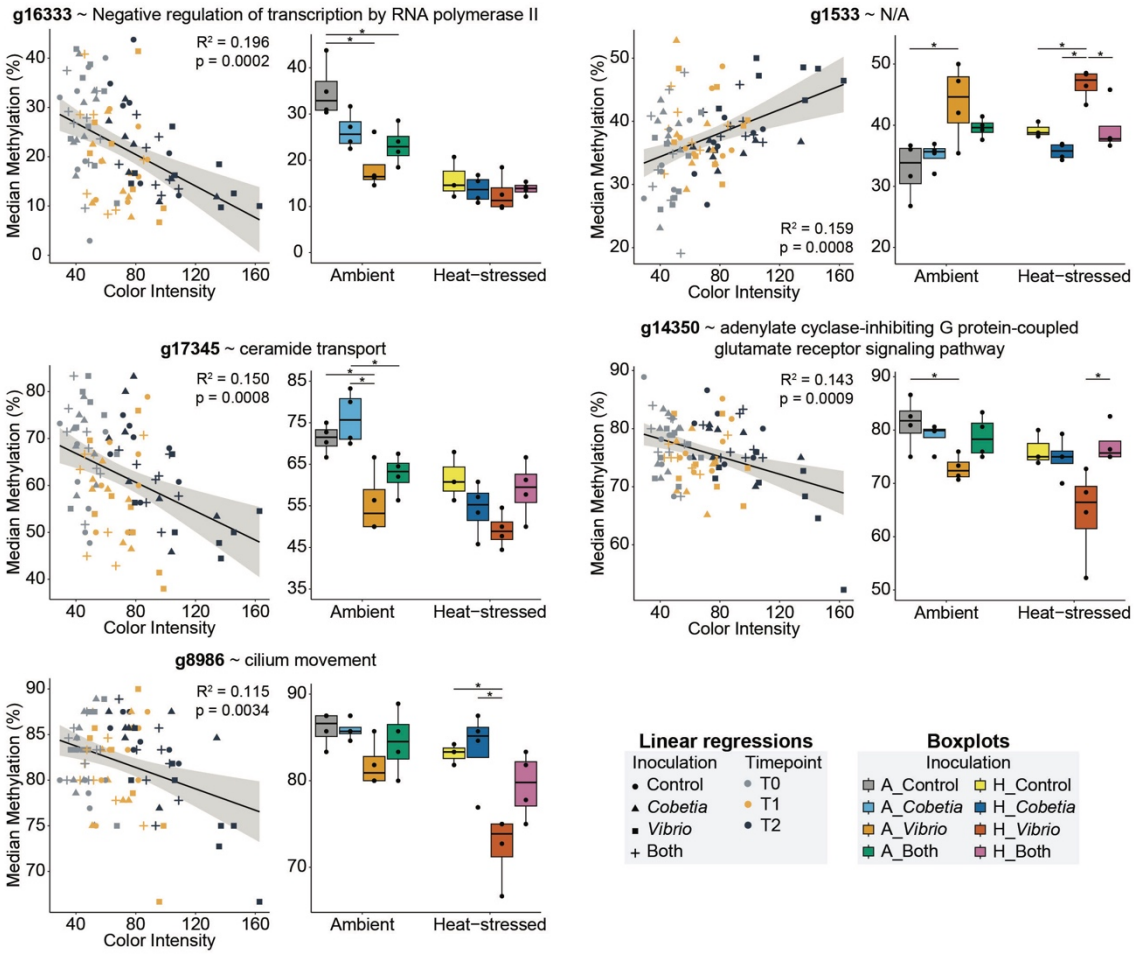

Fig. 5. Methylation profiles of genes with significant correlations ($R^2 > 0.100$, $p < 0.05$) between methylation levels and phenotypic response (coral nubbin color intensity). Linear regression plots show the correlation lines of the coral nubbin color intensity to the median methylation percent in each sample (n = 91) along with the 95% confidence intervals (shaded regions). Boxplots showing the median methylation percent of the samples at T2 (after recovery), were used to compare between groups with one-way ANOVA, followed by TukeyHSD (n = 4; n = 3 for H_Control). Asterisks denote significance between inoculation groups in the boxplots ($p < 0.05$). Boxplots display the individual data points, medians, lower and upper quartiles, and whiskers displaying the 1.5x interquartile range.

Discussion

Although hypothesized, the interaction between changes in the coral-associated microbiome and the coral epigenome was yet to be demonstrated[13,18]. The findings of this

333 study are fourfold, as we show that, in corals, (1) the addition of a single probiotic
334 (*Cobetia* sp.) was able to reduce the indicators of stress caused by inoculation with the
335 pathogen *V. coralliilyticus*; (2) bacterial inoculation, as well as temperature stress,
336 contribute to differences in DNA methylation; (3) gene expression is, on the whole,
337 positively correlated with methylation levels and affected by pathogen and heat stress; (4)
338 pathogen inoculation causes changes in DNA methylation and gene expression to specific
339 cellular processes and immune responses that was mitigated by the probiotic.
340
341 Regarding the phenotypic response, differences in color intensity and tissue loss observed
342 in the coral nubbins at T2 between the control group and the *Vibrio* inoculation in the
343 heat-stressed corals may be a delayed effect of the establishment of the pathogen in the
344 heat-stressed samples at T1. Interestingly, the relative abundances of *V. coralliilyticus*
345 was lower at T2 than T1, coinciding with the observed tissue loss. This result, and the
346 changes to bacterial community diversity indices in heat-stressed nubbins indicate that
347 the holobiont is becoming increasingly dysbiotic[24]. Furthermore, the co-inoculation with
348 the BMC mitigated *Vibrio* establishment in the microbiome during the peak of stress at
349 T1, and controlled the relative abundances of *Vibrio* to similar degree at T2. The co-
350 inoculation also had a positive impact on the phenotype in heat-stressed corals at T2,
351 contributing to the increased stress resilience and survival observed in this group versus
352 the *Vibrio*-inoculated group. Together, this supports the notion that, although heat stress
353 leads to overall changes in the microbial community, attenuation of the pathogen by the
354 addition of probiotics boosts coral resilience.
355

356 DNA methylation has been shown to be responsive to environmental changes[15,17,25-28],
357 correlate with phenotypic acclimatization[15,28], and be heritable[29]. Plasticity of DNA
358 methylation in corals thus far has been tested on the scale of weeks[28,30-32] and
359 months[17,26,27,33] to a year or more[14,15,25,33]. The findings here further prove the plasticity of
360 coral epigenomes during stress, as 12 days of sustained heat stress induced DNA
361 methylation changes across the genome. Furthermore, the difference continued during a
362 nine-day recovery period, which exemplifies persistence of epigenome modifications
363 brought about by environmental change.
364
365 Recently, the concept of "epigenetic memory", where intragenerational differences
366 between epigenomes of different individuals lead to vertical transmission of distinct
367 epigenomes, was confirmed in the brain coral *Platygyra daedalea*[29]. This concept has
368 been recognized in plants for many years (reviewed in [34]). Here, the changes in
369 epigenomes driven by environmental differences as well as bacterial inoculations, signify
370 the potential for long-term persistence after removal of the environmental stress and
371 shows promise for microbiome manipulation experiments with implications for long-term
372 acclimation and coral resilience.
373
374 When analyzing the methylation levels of the genes and putative functions, we can
375 conclude that *Vibrio* inoculation caused changes to methylation levels in metabolic and
376 cellular processes relevant to the observed phenotypic responses (Fig. 1). The difference
377 between the *Vibrio*-inoculated corals and the other three inoculation groups (control,
378 inoculation with *Cobetia* sp., and the co-inoculation) in these genes at T2, independent of

379 the temperature regime, demonstrates the coral probiotic's ability to prevent changes to
380 the coral epigenome in key functions altered by the pathogen (*V. coralliilyticus*). This
381 effect was associated with increased resilience to stress and higher survival rates.
382 Moreover, methylation of functions related to algal symbiosis (e.g., "adenylate cyclase-
383 inhibiting G protein-coupled glutamate receptor signaling pathway" and "lamellipodium
384 morphogenesis") and immune responses (e.g., "early endosome to Golgi transport") were
385 depleted in *Vibrio*-inoculated corals. As mentioned above, pathogen stress may reduce
386 epigenetic control over glutamate receptor pathways, disrupting algal symbiosis and
387 compromising coral health. Glutamate mediates interactions between corals and their
388 algal symbionts[22], and inhibiting glutamate receptors disrupts this relationship[35].
389 Lamellipodia, and by association "lamellipodium morphogenesis", also contributes to
390 coral-algal interactions[36], as well as wound healing in the cnidarian *Clytia*
391 *hemisphaerica*[37]. Reduced methylation of "early endosome to Golgi transport" supports
392 previous findings that *Vibrio* targets endosomal pathways during infection[38]. Specifically,
393 toxins produced by *V. coralliilyticus* disrupt endosome development and downregulate
394 immune genes in the host[38,39]. These methylation changes indicate the *Vibrio*'s ability to
395 elicit a response to coral host defense genes, and the lack of difference between co-
396 inoculated corals and the other inoculations shows the probiotic's ability to mitigate this
397 effect.
398
399 We also confirmed that overall gene expression was positively correlated with gene
400 methylation, which adds to the growing evidence that basal coral epigenomes and gene
401 expression levels are correlated[14,15,31,40]. The correlated down-methylation and down-
402 regulation of genes related to transmembrane transporter activity (g13505), cilium

403 movement (g8986), and negative regulation of transcription by RNA polymerase II
404 (g16333) due to pathogen exposure may indicate direct mechanisms or host responses to
405 the stress. For example, transmembrane transporters are essential for transporting
406 nutrients between corals and their symbionts; reduced expression of related genes may
407 signal a breakdown in symbiosis[41]. The pathogen's impact on cilium movement
408 expression and methylation also shows that the stressed coral nubbins may have been
409 unable to remove excess reactive oxygen species[42], which could have contributed to
410 tissue bleaching and death observed in our samples. RNA polymerase II, on the other
411 hand, helps control spurious transcription by recruiting the histone-methylating enzyme
412 SetD2 to transcribed DNA[14,16]. Therefore, pathogen-induced repression of this gene
413 demonstrates a disruption in both the transcriptional and epigenetic control of gene
414 fidelity. The significant positive correlations between DNA methylation in the latter two
415 genes (g8986 and g16333), as well as in the glutamate receptor pathway gene (g14350),
416 and the coral's phenotypic response to *Vibrio* inoculation further demonstrates the
417 importance of integrating coral epigenomes into coral immune research.
418
419 Despite the association between DNA methylation and gene expression, questions remain
420 about the direction and magnitude of this relationship, and its implications for
421 acclimation and adaptation [31,32]. This has led to the hypothesis that coral gene
422 methylation responds to transcription levels, rather than functioning as a gene regulatory
423 mechanism like it does in mammals [14,27,32]. Thus, epigenomes may help to explain how
424 rapid gene expression changes caused by pathogen stress lead to long-term phenotypic
425 responses.

426

427 The direct mechanisms by which bacteria are able to elicit changes to the coral
428 epigenome are still to be explored, although metabolites and proteins produced by coral-
429 associated bacteria are suggested to play a role[13,18]. Additionally, the crosstalk between
430 coral epigenomes and coral-associated bacteria may not be unidirectional, as pathogen
431 susceptibility has been hypothesized to be at least partly controlled by epigenetic factors
432 in aquaculture fish[43]. By connecting rapid microbiome changes to more long-term and
433 heritable epigenetic changes (Fig. 6), bacteria inoculation has the potential to induce
434 lasting differences, even without direct establishment in the bacterial community. Thus,
435 as future studies explore this interaction further, the current paradigm that microbiome
436 interventions only lead to short-term and volatile changes[44] might shift. Therefore, as
437 research in this field progresses, there is considerable potential to shape the use of
438 customized microbial therapies for increasing resistance and resilience in vulnerable
439 corals[45,46].

440

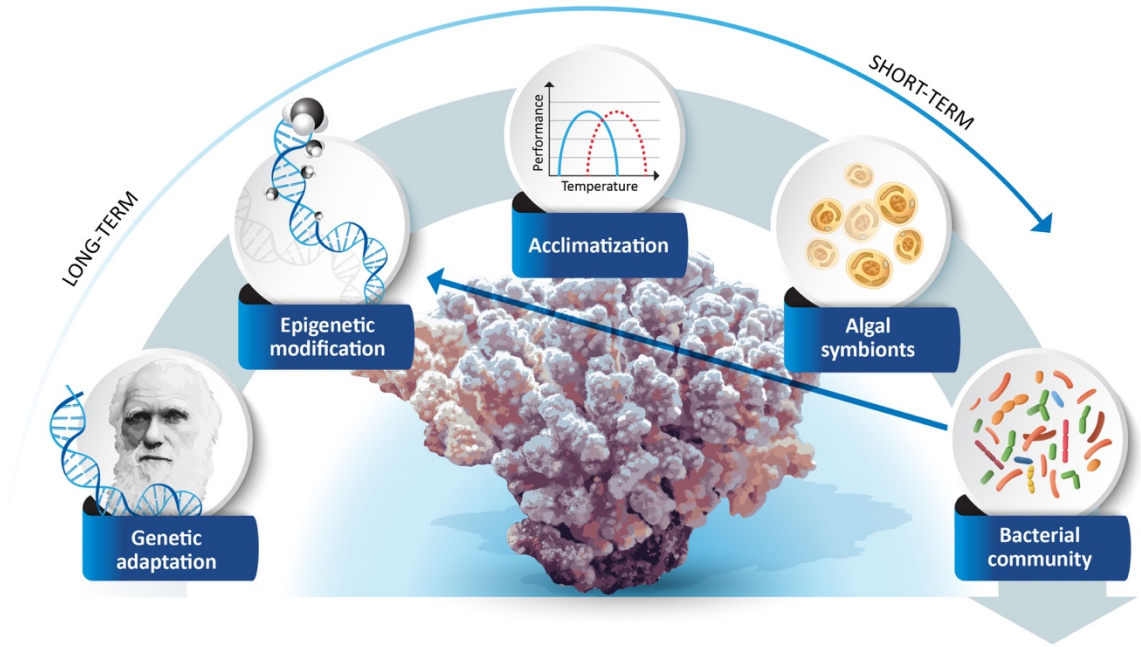

Fig. 6. Rethinking the flexibility and longevity of coral microbiomes via crosstalk with coral epigenomes. Microbiome changes occur quickly and are fleeting. However, relating microbiome manipulation and coral DNA methylation here shows that bacterial community changes may induce long-term and possibly heritable changes in corals by influencing modifications to the coral epigenome. This figure highlights the transformative nature of our results by adding an arrow to the previous concept postulated in ref.[47], connecting the bacterial community with epigenetic modification.

453 **Methods**

454

455 ***Coral collection and experimental setup***

456

457 In order to prevent intergenomic variability would obfuscate identification of methylation
458 marks[48], clonal fragments from *Pocillopora verrucosa* were collected from the Al Fahal
459 reef in the central Red Sea (22˚ 18.3071' N, 38˚ 57.8741' E) on 14 March 2022 (*in situ*
460 seawater temperature = 25˚C) and brought to the aquariums at the Coastal and Marine
461 Resources Core Lab (CMR) in King Abdullah University of Science and Technology
462 (KAUST). All coral husbandry and experimentation was done under the supervision of
463 KAUST's Institutional Biosafety and Bioethics Committee (IBEC). The coral colony was
464 acclimated to CMR conditions (using a 300 L open-system aquarium tank, with a
465 maximum intensity of 180 µmol of photons m−2 s−1 between 10:00 to 14:00, and a 12-
466 hour day/night cycle changing at 7:00 and 19:00) and brought to 27˚C over the course of
467 three weeks (approximately 0.5˚C increase every two days, followed by two weeks at
468 27˚C). Corals were further fragmented into finger-sized nubbins on 4 April 2022. After a
469 five-week recovery period, nubbins were divided into the eight experimental tanks which
470 housed the replicates for each inoculation group (10 L aquarium tanks, using the same
471 light parameters as the acclimation tank above) containing 0.22 µm filtered seawater. The
472 coral nubbins were acclimated for seven days (until the average *Fv/Fm* ratio, a measure
473 for photosynthetic efficiency and proxy for coral health, from the coral nubbins in each
474 experimental tank was >0.600, using a Diving-PAM II; Walz, Germany).

475

476 The bacteria used in the experiment were the BMC *Cobetia* sp. strain pBMC4 (isolated
477 from *Pocillopora verrucosa*[19]) and the opportunistic pathogen *Vibrio coralliilyticus* strain
478 BAA-450 (isolated from *Pocillopora damicornis*[20]). The bacteria cultures used in this
479 experiment were grown using Marine Broth 2216 (Becton Dickinson, USA) for 24 hours
480 at 27˚C before each inoculation. To minimize additional carbon input from the culture
481 media, the cultures were spun at 6000 x g for 5 min and the bacteria pellets were
482 resuspended in sterilized 3.5% NaCl solution. This process was repeated for a total of two
483 washes, then the bacteria were resuspended in sterilized 3.5% NaCl solution for
484 inoculation. Abundance and purity of each of the cultures were checked by the plate
485 counting method using Marine Agar 2216 (Becton Dickinson, USA).
486
487 Starting on day 1, bacteria were inoculated into each of the tanks every three days at a
488 final concentration of 10^5 cells/mL. Thirty percent of the water was replaced with new
489 0.22 µm filtered seawater (kept at the same temperature of the experimental tanks) every
490 other day. The experiment was performed over 28 days. Of the eight experimental tanks,
491 four were maintained at 27˚C throughout the entirety of the experiment (denoted with an
492 "A" for ambient temperature). In the other four experimental tanks, starting from day 1,
493 temperature was increased from 27˚C to 33˚C (by increasing the temperature 1˚C per day
494 for 6 days), then maintained at 33˚C for 12 days (until the average *Fv/Fm* across all
495 conditions was <0.450), then returned to 27˚C (by decreasing the temperature 1˚C per
496 day) where they were kept until the end of the experiment (4 days). These tanks are
497 denoted with an "H" for heat stress. The four experimental tanks in each of A or H,
498 contained one of the following experimental conditions: corals with no inoculation

499 ("Control"), corals inoculated with *Cobetia* sp. at a final concentration of 10^5 cells/mL
500 ("*Cobetia*"), corals inoculated with *V. coralliilyticus* at a final concentration of 10^5
501 cells/mL ("*Vibrio*"), and corals inoculated with both *Cobetia* sp. and *V. coralliilyticus*,
502 each at a final concentration of 10^5 cells/mL ("Both"). In total the eight conditions were:
503 A_Control, A_*Cobetia*, A_*Vibrio*, A_Both, H_Control, H_*Cobetia*, H_*Vibrio*, and
504 H_Both.
505
506 Samples of four coral nubbin replicates (n = 4) per tank were taken at the start of the
507 experiment before any bacterial inoculation (T0), on day 19 (peak of stress, T1), and on
508 day 28 (after recovery, T2). At each sampling time, the apical tip of the sampled nubbin
509 was removed and flash frozen in liquid nitrogen for nucleic acid analysis. Frozen nubbins
510 were then transferred to -80˚C until processing.
511
512 ***Coral health parameters***
513
514 Coral health was monitored during the experiment using a Diving-PAM II (Walz,
515 Germany) to measure the *Fv/Fm* ratios. *Fv/Fm* measurements were taken after dark
516 acclimating the coral nubbins for at least 1 hour the night before each inoculation day
517 (every three days starting on day 0) throughout the entirety of the experiment (n = 4 for
518 each experimental tank). *Fv/Fm* measurements were compared between temperature
519 groups using Wilcoxon Rank Sum tests[49], and between inoculation groups Kruskal-
520 Wallis H tests[50]. Images were taken of the coral nubbins at T0 and at their respective
521 sampling times (T1 or T2).

522

523 ImageJ was used to analyze the percent live tissue, color intensity, and color intensity of
524 live tissue of each of the images of the nubbins from sampling times T0 (n = 12 for each
525 group), T1 (n = 4 for each group), and T2 (n = 4 for each group). For the percent live
526 tissue, the area of live tissue on the coral nubbin was divided by the total area of the coral
527 nubbin in each respective image. The color intensity, as described in the main text, was
528 obtained using the unweighted average in color intensity for each coral nubbin, after
529 converting the image to 8-bit grayscale (offering $2^8 = 256$ levels of differentiation). The
530 average color intensity incorporates the color intensities (from 0 = black, to 256 = white)
531 of all pixels within a coral nubbin. This, then, incorporates the color of the live tissue and
532 any exposed coral skeleton that may be present in coral nubbins with tissue loss. For the
533 color intensity of live tissue, only the unweighted average in color intensity observed in
534 the live tissue portion of the image was considered. Percent live tissue, color intensity,
535 and color intensity of live tissue measurements were compared between the samples with
536 Kruskal-Wallis H tests[50], followed by Dunn's multiple comparison test[51] using
537 Benjamini-Hochberg adjustment.

538

539 ***16S rRNA gene amplicon sequencing***

540

541 DNA and RNA were extracted from airbrushed coral tissue using AllPrep DNA/RNA
542 Mini Kit (Qiagen, Germany), following manufacturer's instructions. Extracted DNA was
543 used for analysis of the bacterial community as well as identification of the methylation
544 marks within the coral genome. For bacterial community analysis, the DNA composing

545 the V3-V4 region of the 16S rRNA gene was sent to Novogene (Novogene, China) for
546 sequencing using a NovaSeq 6000 (Illumina, USA) with the primers 341F (5'-
547 CCTAYGGGRBGCASCAG-3') and 806R (5'-GGACTACNNGGGTATCTAAT-3').
548
549 ***Library preparation and sequencing of methylated DNA***
550
551 Libraries of converted methylated DNA were prepared using the NEB Enzymatic
552 Methyl-seq Kit (New England Biolabs Inc., USA) with the EM-seq Index Primers (New
553 England Biolabs Inc., USA). Prepared libraries were sent to Novogene (Novogene,
554 China) for sequencing using a NovaSeq 6000 (Illumina, USA). Due to insufficient DNA
555 quality in 5 samples, 91 of the 96 samples were used for downstream analysis (n = 4 for
556 each experimental group; except A_Control at T1; H_Control at T0, T1, and T2; and
557 H_Both at T1; which all had n = 3).
558
559 ***Coral microbiome analysis***
560
561 For microbiome analysis, primer sequences were removed using cutadapt[52]. Sequences
562 were further filtered and trimmed using the DADA2 pipeline[53]. Taxonomy was assigned
563 using the SILVA_nr99_v138.1 database[54]. Sequences identified as Bacteria that did not
564 match to Chloroplast or Mitochondria were further analyzed using phyloseq[55]. ASVs with
565 a 100% match to the 16S rDNA sequence of the inoculums (*Cobetia* sp. or *Vibrio*
566 *coralliilyticus*) via BLASTN[56] were determined to be representative ASVs of the
567 inoculated bacteria. Statistical differences between relative abundance data in different

568 groups were determined using the *vegan* package in R (version 4.3.1). Bacterial
569 abundances were not normally distributed (*Shapiro-Wilk*: $p < 0.05$), so significant
570 differences between groups were determined by non-parametric tests. Kruskal Wallis H
571 tests[50], followed by Dunn's multiple comparison tests[51], were used to find significant
572 differences between inoculation groups (n = 4 for each experimental group).
573
574 Microbiome composition differences were calculated between inoculation groups in each
575 of the temperature conditions and timepoints using principal coordinate analyses (PCoA).
576 Significant factors driving the separation between samples and sample dispersion were
577 determined using the adonis2 and betadisper commands in the *vegan* R package (version
578 4.3.1). Pairwise differences between inoculation groups were tested using the
579 pairwise.adonis command in the *pairwiseAdonis* R package.
580
581 ***Coral DNA methylation***
582
583 DNA methylation was analyzed bioinformatically following the steps described in Liew
584 et al. (2020)[29]. Reads were first trimmed using TrimGalore v0.6.10[52]. Then, the filtered
585 reads were mapped to a reference genome for *Pocillopora verrucosa*[57] and deduplicated,
586 before methylation marks were scored per-position using Bismark v0.23.1[58]. Methylated
587 DNA positions were only considered bona fide if they met the criteria defined in Liew et
588 al. (2020)[29]. Briefly, the probability of methylated positions resulting from sequencing
589 error needed to be below 0.05 after correcting for false discovery rate, and the methylated
590 reads were only kept if the methylation occurred in all replicates of at least one of the

591 experimental conditions. Also, to minimize type I errors, the median coverage needed to
592 be ≥ 10 and minimum coverage needed to be ≥ 5 across all of the samples in order to be
593 considered for further analyses[14,15,29] (Supplementary Table 11).
594
595 The median methylation levels across genes were compared between groups. Each
596 methylated position within a given gene was given a score between 0 (no methylation in
597 any of the cells) to 1 (fully methylated across all cells), and the median across each gene
598 was used for further analyses. Only genes with five or more methylated positions were
599 used for downstream analyses. Nonmetric multidimensional scaling (nMDS) plots were
600 used to compare the median methylation across the genome of the coral using Bray-
601 Curtis dissimilarity to separate samples. Significant factors driving the separation
602 between samples and sample dispersion were determined by PERMANOVA using the
603 adonis2 and PERMDISP using betadisper commands in the *vegan* R package (version
604 4.3.1). Pairwise differences between groups were tested using the pairwise.adonis
605 command in the *pairwiseAdonis* R package.
606
607 To extrapolate the genes related to the difference observed between the Control
608 inoculation and the *Vibrio*-treated corals at T2, generalized linear models (GLMs) were
609 implemented in R using the following formula:
610 glm(median_methylation_levels ~ temperature + inoculation, family = gaussian())
611 for the data from T2, where median methylation levels for each gene was compared with
612 the predictor variables temperature (ambient vs. heat-stressed) and inoculation (by using
613 the Control inoculation as a baseline to compare with each of *Cobetia*-treated, *Vibrio*-

614 treated, and the co-inoculation inoculation samples). Genes with fewer than 5 methylated
615 positions were removed from the analysis. Genes with *Vibrio* inoculation as a significant
616 predictor variable (after correcting for false discovery rate) were plotted on a heatmap
617 with all of the T2 samples using hierarchical clustering with Euclidean distances and the
618 "ward.D2" agglomeration method.
619
620 ***Functional enrichment of differently methylated genes***
621
622 GO term annotations were collected from the published *P. verrucosa* genome[57]. GO term
623 enrichment analysis was performed using TopGO[59] on the genes with significantly
624 different methylation levels from the previous step. Enriched GO terms with $p < 0.05$ and
625 were considered significant.
626
627 ***RNA-Seq analysis***
628
629 T2 RNA samples (n = 32) extracted using the AllPrep DNA/RNA Mini Kit (Qiagen,
630 Germany) were lyophilized onto a GenTegraRNA plate (Gentegra, USA) and sent to the
631 MR DNA (Molecular Research LP, USA) for RNA-seq analysis. There, the lyophilized
632 RNA was resuspended in 30uL RNase free water, and 500-750 ng of total RNA was used
633 for library preparation using the poly-A selection method of KAPA mRNA HyperPrep
634 Kits (Roche, Switzerland) following the manufacturer's instructions. The libraries were
635 then pooled in equimolar ratios of 0.6 nM and sequenced using a NovaSeq 6000
636 (Illumina, USA). RNA-seq reads were first trimmed using TrimGalore v0.6.10[52]. The

637 adapter-trimmed reads were pseudo-aligned to *P. verrucosa* gene models[57] using kallisto
638 v0.50.1[60] to quantify gene expression levels. Transcripts per million (TPM) obtained
639 from sleuth v0.30.1[61] were then used to compare across inoculation and temperature
640 groups from T2 (n = 4 for each condition). Correlations between TPM and median
641 methylation levels across genes were determined using the linear model:

642 $$lm(log_2(TPM + 1) \sim median_methylation_levels, data = gene)$$

643 Significant correlations in individual genes were determined using Benjamini-Hochberg
644 adjusted p-values. Gene expression levels across the T2 samples were then compared
645 pairwise between the temperature groups (n = 16 per temperature regime) and inoculation
646 groups (n = 8 per inoculation group).
647
648 ***Correlating median methylation with phenotypic parameters***
649
650 The genes predicted to be associated with *Vibrio* inoculation in the previous step were
651 then tested against a phenotypic response variable using linear models with the formula:

652 $$lm(median_methylation_levels \sim color_intensity, data = gene)$$

653 to determine which of these genes correlated with phenotypic differences observed in the
654 corals affected by temperature and inoculation. The genes with $R^2 > 0.100$ and $p < 0.05$
655 (after Benjamini-Hochberg correction) were plotted using linear regressions with 95%
656 confidence intervals. Boxplots showing the median methylation levels of these genes in
657 each sample at T2 were then used to compare differences between groups using one-way
658 ANOVA followed by TukeyHSD.
659

660 **Data availability**

661

662 EM-seq data is deposited in the NCBI Sequence Read Archive under the BioProject

663 accession number PRJNA1123499 (https://www.ncbi.nlm.nih.gov/sra/PRJNA1123499).

664

665 **Code availability**

666

667 The code used for data analysis can be found at: https://github.com/arbarno/pver_epibac.

668 **Acknowledgements**

669

670 We would like to thank the Coastal and Marine Resources Lab and Bioscience Core Lab

671 for their support and assistance throughout the experiment. This work was supported by

672 KAUST grant number BAS/1/1095-01-01

673

674 **Author contributions**

675

676 A.R.B., H.D.M.V., G.C., T.T., M.A., C.R.V., and R.S.P. designed the experiments;

677 A.R.B., H.D.M.V., P.M.C. conducted the mesocosm experiment and sample collection;

678 A.R.B. and N.D. performed DNA extractions; A.R.B. and F.C.G. performed analyses;

679 A.R.B. wrote the manuscript with input from all authors; A.S.R. and R.S.P. provided

680 guidance and funding during the experiment.

681

682 **Competing interests**

683

684 The authors declare no conflicting interests.

685

686 **Materials & Correspondence**

687

688 Correspondence to Adam R. Barno or Raquel S. Peixoto.

689

690 **Supplementary Information**

691

692 Supplementary tables are provided in excel format.

693

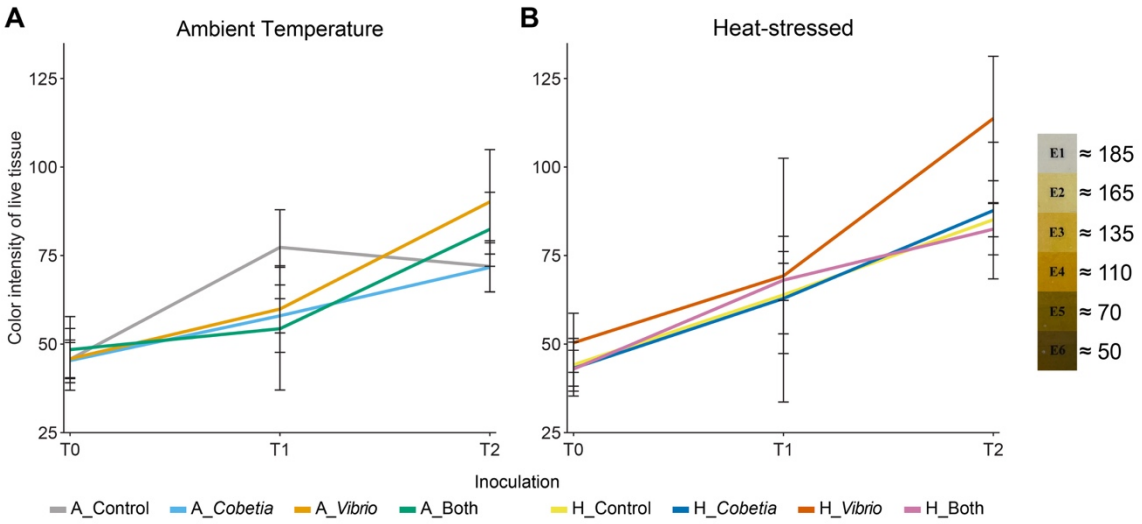

Extended Data Fig. 1. Color intensity of live tissue for the coral nubbins throughout the experiment. Lines represent the mean color intensities are plotted for each bacterial inoculation group at each timepoint for nubbins in the (A) ambient temperature condition and (B) heat-stressed condition, as measured by ImageJ (T0: n = 12 per group; T1/T2: n = 4 per group). The error bars represent standard deviations. Color intensity was measured on the CoralWatch Coral Health Chart[21] for reference.

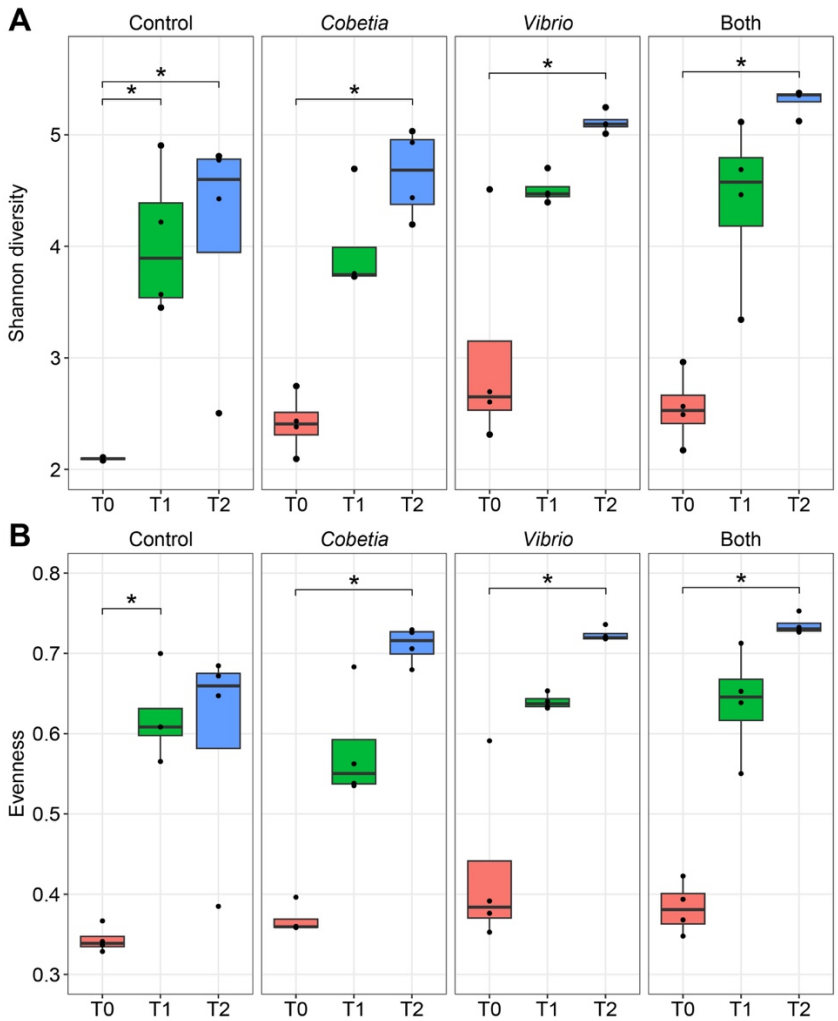

Extended Data Fig. 2. Alpha diversity indices from the microbiomes of the heat-stressed samples, separated by bacteria inoculation and timepoint. The y-axes represent (A) the alpha diversity measured using Shannon diversity and (B) the evenness within each sample, measured using the Pielou index. Samples were compared across timepoints within each inoculation group using Kruskal Wallis H tests, followed by Dunn's multiple comparison tests (n = 4 for each group). Significant differences ($p < 0.05$, after Benjamini-Hochberg correction) are denoted with asterisks.

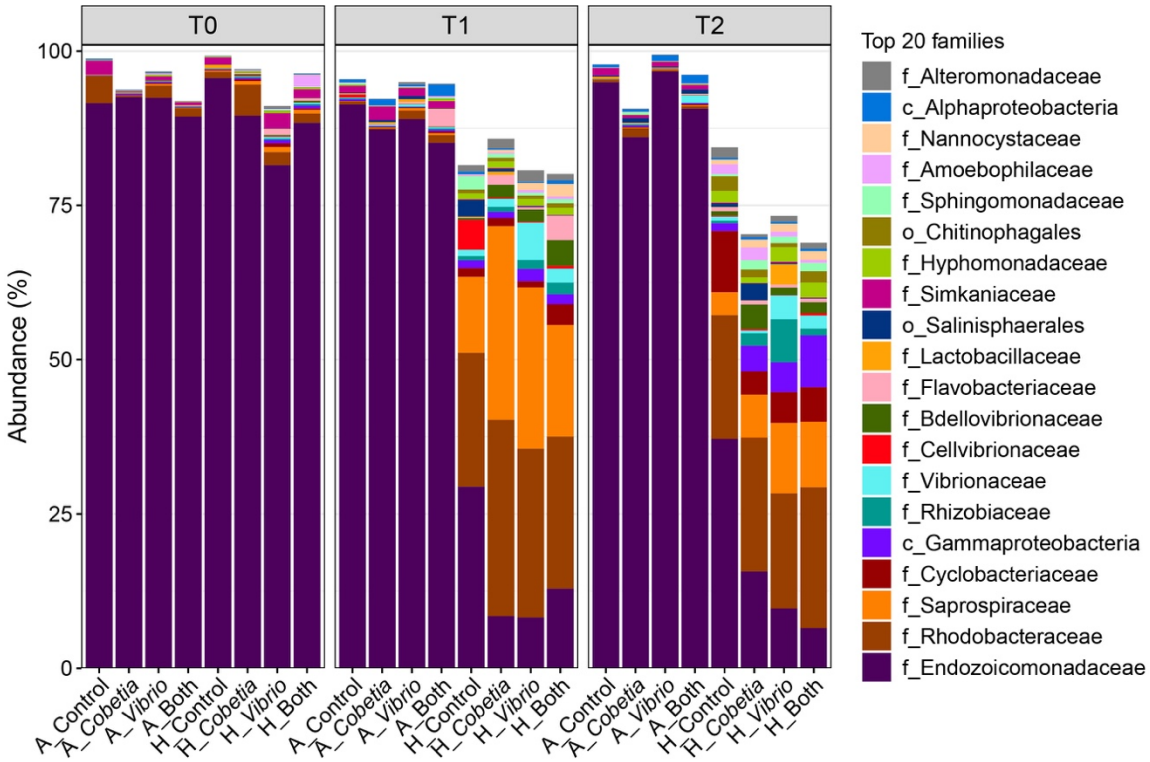

Extended Data Fig. 3. The top 20 most abundant bacterial families within the samples are represented as stacked barcharts for each experimental group, separated by timepoint (n = 4 per group). The y-axis is the relative abundance for each bacterium within the sample group. For the bacteria, where the family was not identified, the lowest taxonomic identification is listed ("f_" = family, "c_" = class, "o_" = order).

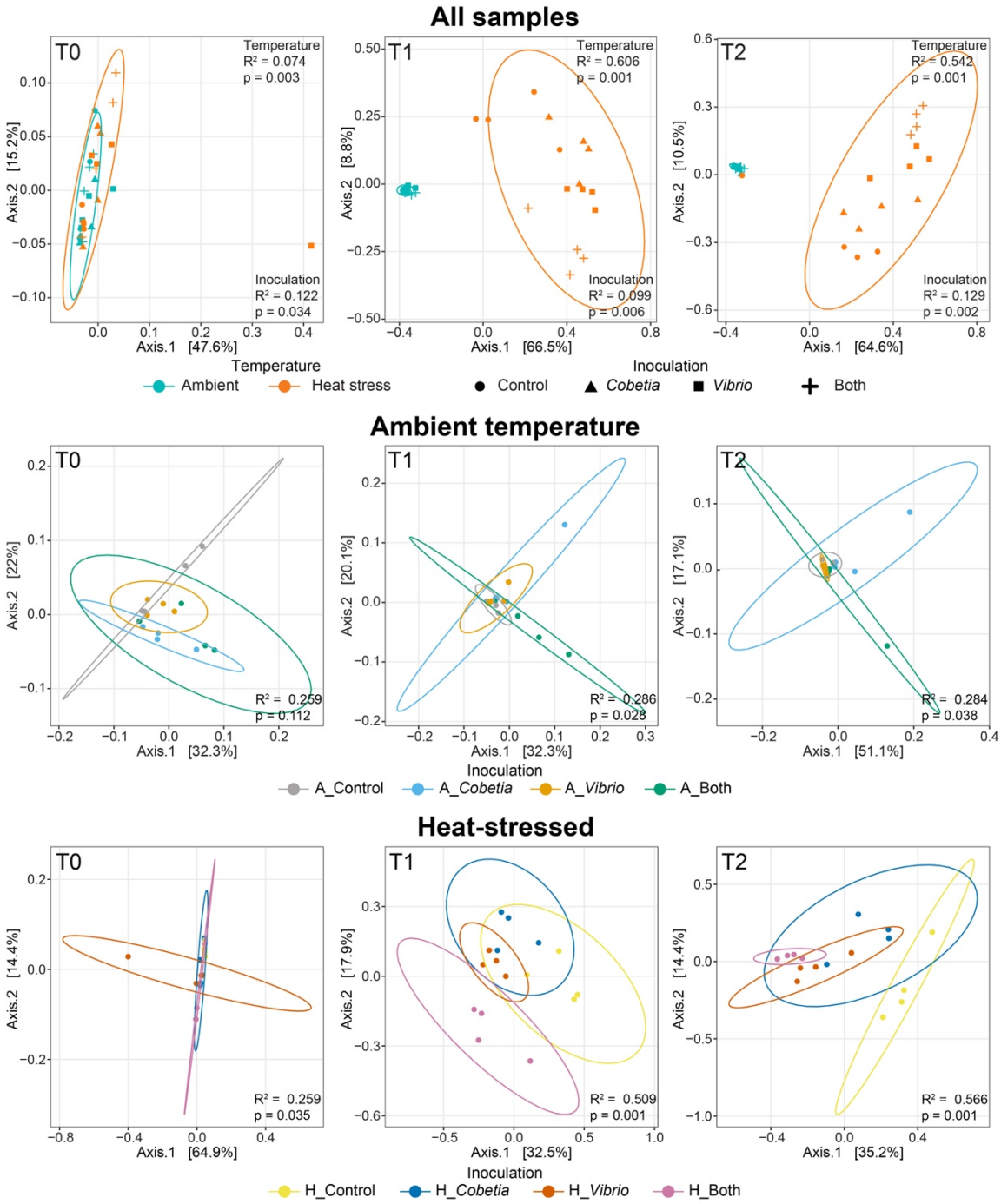

Extended Data Fig. 4. Principle coordinate analysis (PCoA) plots based on Bray-Curtis dissimilarities of the relative abundances of the total bacterial community in the coral nubbins at each sampling time. Samples from each timepoint were separated using Bray-Curtis dissimilarity and plotted along the first two dimensions (n = 4 per group). Circles = 95% confidence intervals around temperature groups. Both temperature and inoculation were tested as factors driving the separation between groups using PERMANOVA (top row). For each temperature regime (ambient – middle row and heat-stressed – bottom row), significant differences between

731 inoculation were tested using PERMANOVA. R^2 and p-values are displayed, representing the
732 magnitude and significance attributed to each of the factors.
733
734
735

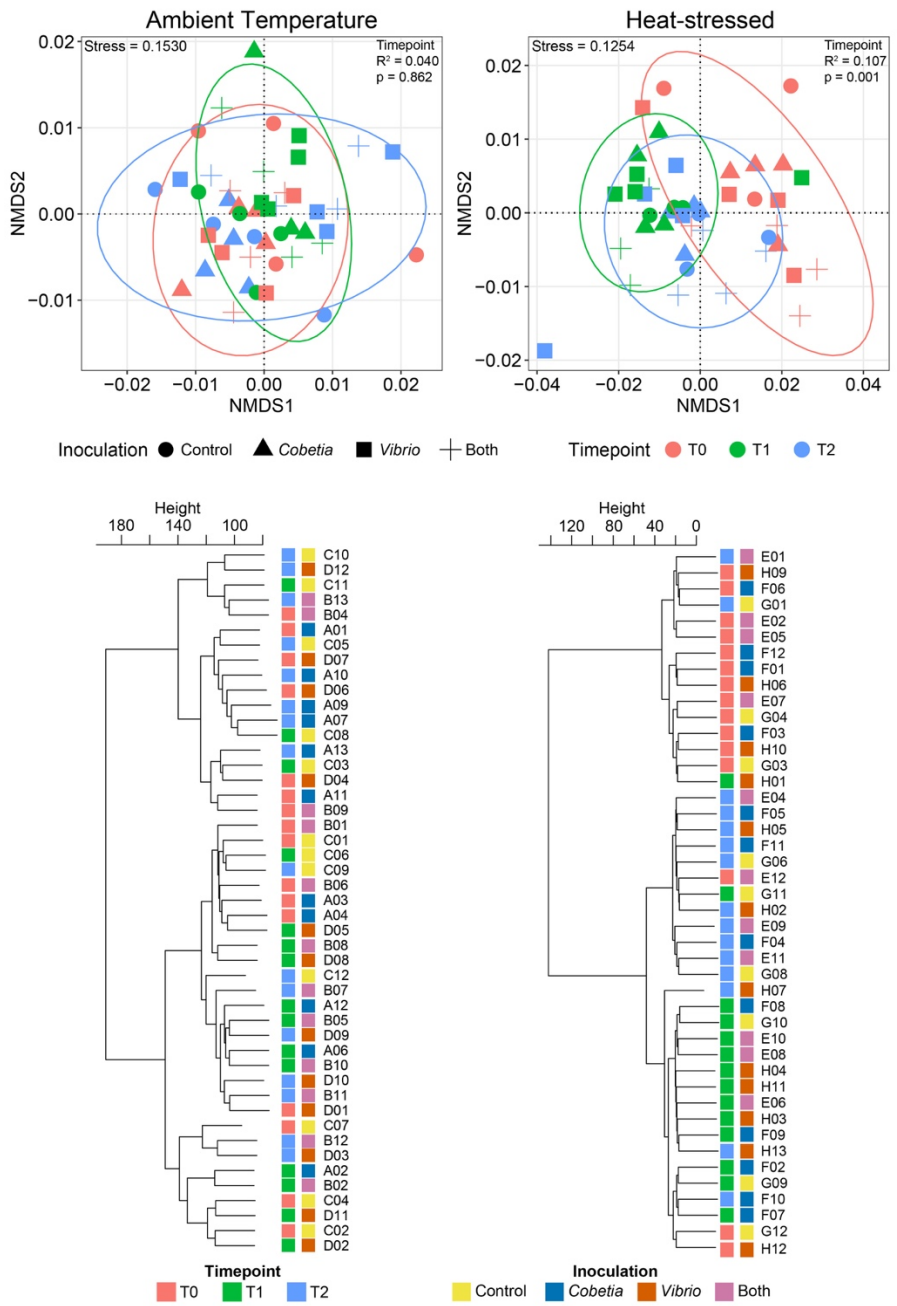

Extended Data Fig. 5. Separation of genome-wide DNA methylation in samples based on timepoint in ambient temperature corals and heat-stressed corals via nMDS plots using Bray-Curtis dissimilarity and hierarchical clustering using the "ward.D2" agglomeration method. Circles in nMDS plots = 95% confidence intervals around timepoints. For each temperature regime (ambient – left and heat-stressed – right), significant differences between timepoints were tested using PERMANOVA (Ambient Temperature, T0/T2: n = 16 and T1: n = 15; Heat-stressed, T0/T2: n = 15 and T1: n = 14). R^2 and p-values are displayed, representing the magnitude and significance attributed to each of the factors. Hierarchical clustering demonstrates the relative dissimilarity between clusters of samples based on methylation levels across the genome (represented by dendrogram height).

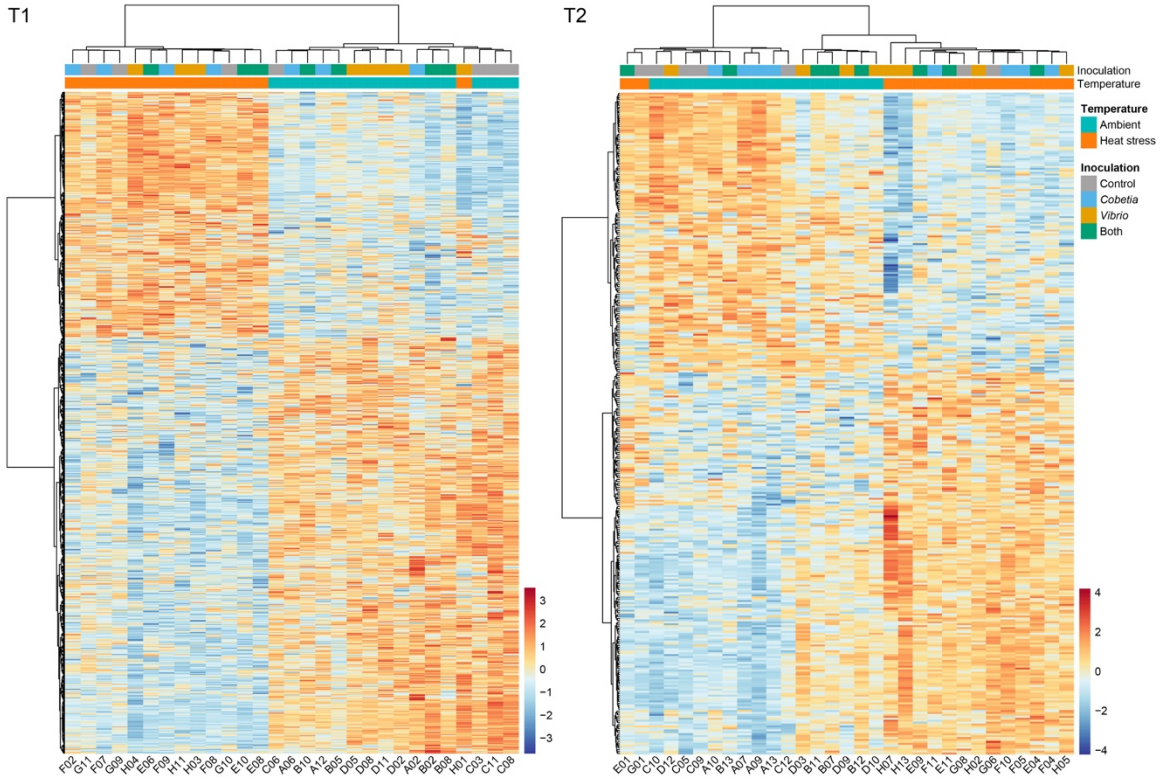

Extended Data Fig. 6. Percent methylation levels of genes significantly driven by temperature conditions (ambient vs. heat stress) at sampling times T1 (left) and T2 (right) as determined by GLMs (n = 4; n = 3 for H_Control at T1/T2; n = 3 for H_Both at T1). Hierarchical clustering was performed using Euclidean distances and the "ward.D2" agglomeration method. Colors represent the z-score for any given gene. All enriched GO terms due to differences in temperature regimes at T1 and T2 are in Supplementary Table 6a and 6b, respectively.

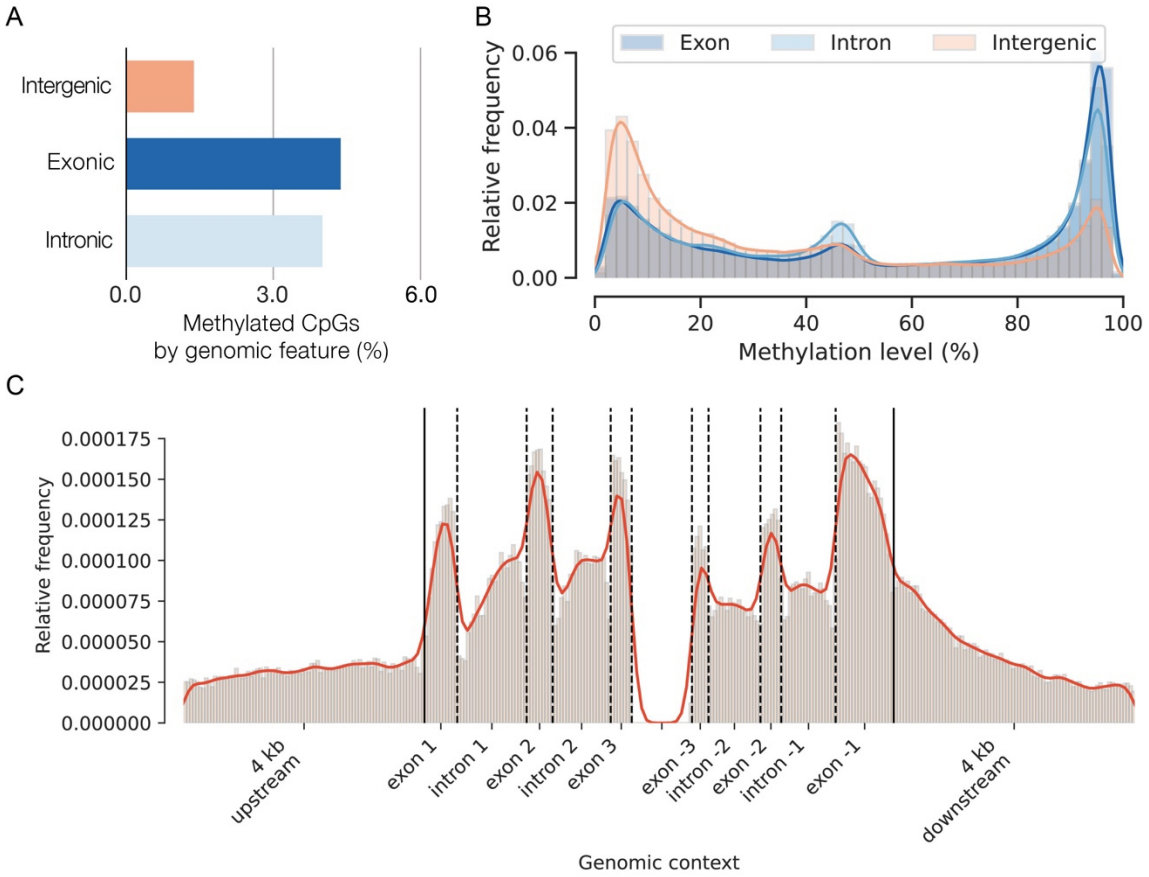

Extended Data Fig. 7. Genomic context of methylation across genomic regions and along genes. Data from all samples (n = 91) were pooled to find where DNA methylation is observed along the *Pocillopora verrucosa* genome. (A) Percent methylated CpGs in each genomic feature group. (B) Methylation levels display approximate bimodal distribution, with higher methylation levels in genic regions (exons and introns) than intergenic regions. (C) The relative frequencies of methylated positions along a standardized gene model show than methylated positions are more frequent within exons.

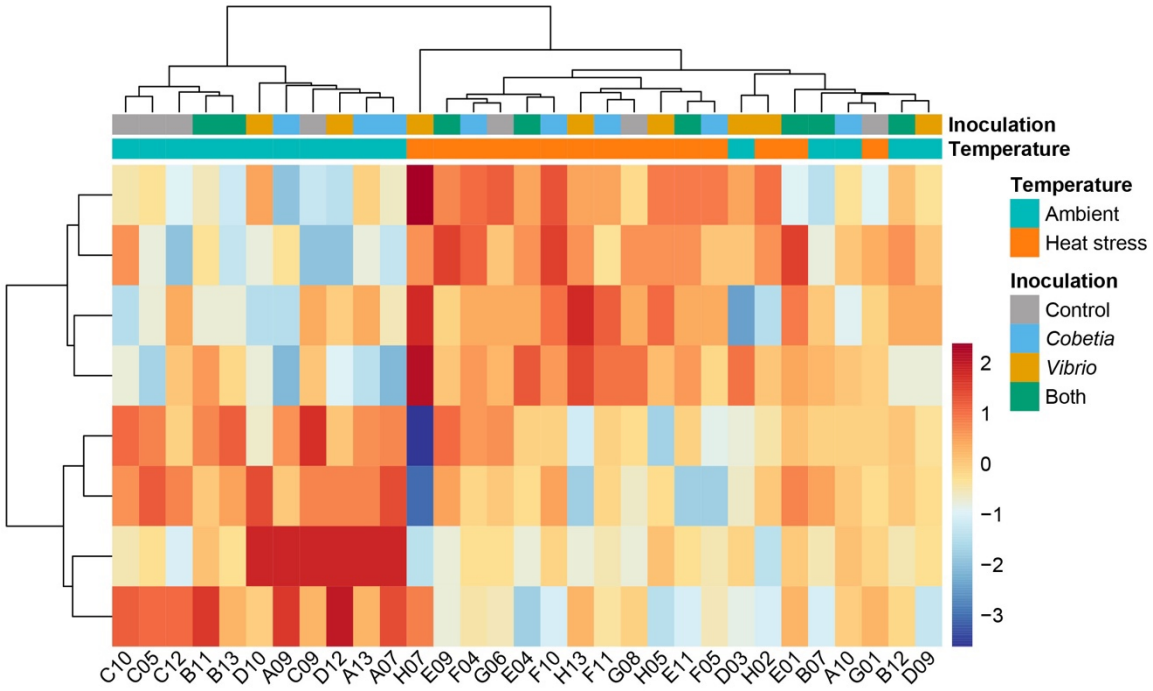

Extended Data Fig. 8. Percent methylation levels of glutamatergic synapse genes significantly driven by temperature conditions (ambient vs. heat stress) at T2 (8 genes total) as determined by GLMs (n = 4; n = 3 for H_Control). Hierarchical clustering was performed using Euclidean distances and the "ward.D2" agglomeration method. Colors represent the z-score for any given gene.

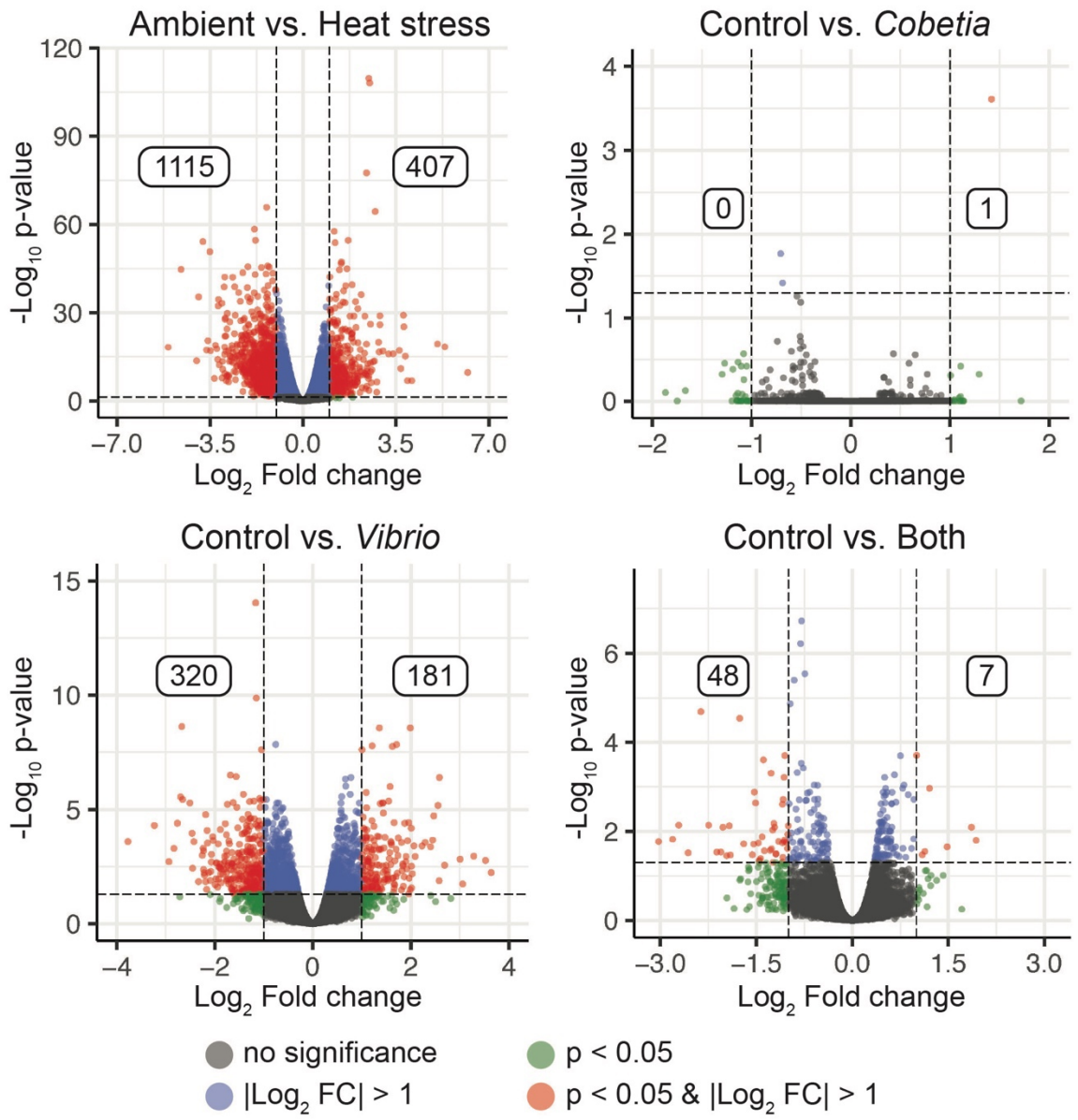

Extended Data Fig. 9. Volcano plots displaying fold-change comparisons from RNA-seq data between the temperature conditions (ambient vs. heat stress; n = 16) and each of the inoculation groups to the control group (n = 8). Each dot within the volcano plots represents the normalized count of a gene. Significantly up-regulated or down-regulated genes in comparison to the ambient temperature (in the temperature comparison) or the control group (in the inoculation comparisons) was determined by a $\log_2$ fold change >1 or <-1 and a $p < 0.05$ after adjusting for false discovery rate.

781 **References**

782 1. Doering, T. et al. Towards enhancing coral heat tolerance: a "microbiome
783 transplantation" treatment using inoculations of homogenized coral tissues.
784 *Microbiome* **9**, 102 (2021)
785 2. Fragoso ados Santos, H. et al. Impact of oil spills on coral reefs can be reduced by
786 bioremediation using probiotic microbiota. *Sci. Rep.* **5**, 18268 (2015)
787 3. Moradi, M. et al. Probiotics mitigate thermal stress- and pathogen-driven impacts on
788 coral skeleton. *Front. Mar. Sci.* **10**, 1212690 (2023)
789 4. Rosado, P. M. et al. Marine probiotics: increasing coral resistance to bleaching
790 through microbiome manipulation. *ISME J.* **13**, 921–936 (2019)
791 5. Santoro, E. P. et al. Coral microbiome manipulation elicits metabolic and genetic
792 restructuring to mitigate heat stress and evade mortality. *Sci. Adv.* **7**, eabg3088 (2021)
793 6. Silva, D. P. et al. Multi-domain probiotic consortium as an alternative to chemical
794 remediation of oil spills at coral reefs and adjacent sites. *Microbiome* **9**, 118 (2021)
795 7. Ushijima, B. et al. Chemical and genomic characterization of a potential probiotic
796 treatment for stony coral tissue loss disease. *Commun. Biol.* **6**, 248 (2023)
797 8. Peixoto, R. S., Rosado, P. M., Leite, D. C. de A., Rosado, A. S. & Bourne, D. G.
798 Beneficial Microorganisms for Corals (BMC): Proposed Mechanisms for Coral
799 Health and Resilience. *Front. Microbiol.* **8**, 341 (2017)
800 9. Reshef, L., Koren, O., Loya, Y., Zilber-Rosenberg, I. & Rosenberg, E. The Coral
801 Probiotic Hypothesis. *Environ. Microbiol.* **8**, 2068–2073 (2006)
802 10. Rohwer, F., Seguritan, V., Azam, F. & Knowlton, N. Diversity and distribution of
803 coral-associated bacteria. *Mar. Ecol. Prog. Ser.* **243**, 1–10 (2002)
804 11. Zhang, Y. et al. Shifting the microbiome of a coral holobiont and improving host
805 physiology by inoculation with a potentially beneficial bacterial consortium. *BMC*
806 *Microbiol.* **21**, 130 (2021)
807 12. Sweet, M. J. & Bulling, M. T. On the Importance of the Microbiome and Pathobiome
808 in Coral Health and Disease. *Front. Mar. Sci.* **4**, 9 (2017)
809 13. Barno, A. R., Villela, H. D. M., Aranda, M., Thomas, T. & Peixoto, R. S. Host under
810 epigenetic control: A novel perspective on the interaction between microorganisms
811 and corals. *BioEssays* **43**, 10 (2021)

812 14. Li, Y. et al. DNA methylation regulates transcriptional homeostasis of algal
813 endosymbiosis in the coral model Aiptasia. *Sci. Adv.* **4**, 8 (2018)
814 15. Liew, Y. J. et al. Epigenome-associated phenotypic acclimatization to ocean
815 acidification in a reef-building coral. *Sci. Adv.* **4**, 6 (2018)
816 16. Neri, F. et al. Intragenic DNA methylation prevents spurious transcription initiation.
817 *Nature* **543**, 72–77 (2017)
818 17. Rodriguez-Casariego, J. A., Cunning, R., Baker, A. C. & Eirin-Lopez, J. M.
819 Symbiont shuffling induces differential DNA methylation responses to thermal stress
820 in the coral *Montastraea cavernosa*. *Mol. Ecol.* **31**, 588–602 (2021)
821 18. Putnam, H. M. Avenues of reef-building coral acclimatization in response to rapid
822 environmental change. *J. Exp. Biol.* **224**, jeb239319 (2021)
823 19. Raimundo, I., Rosado, P. M., Barno, A. R., Antony, C. P. & Peixoto, R. S. Unlocking
824 the genomic potential of Red Sea coral probiotics. *Sci. Rep.* **14**, 14514 (2024)
825 20. Ben-Haim, Y. et al. *Vibrio coralliilyticus* sp. nov., a temperature-dependent pathogen
826 of the coral *Pocillopora damicornis*. *Int. J. Syst. Evol. Microbiol.* **53**, 309–315 (2003)
827 21. Siebeck, U. E., Logan, D. & Marshall, N. J. CoralWatch – a flexible coral bleaching
828 monitoring tool for you and your group. *Coral Reefs.* (2010)
829 22. Cui, G. et al. Host-dependent nitrogen recycling as a mechanism of symbiont control
830 in *Aiptasia*. *PLOS Genet.* **15**, e1008189 (2019)
831 23. Rädecker, N. et al. Heat stress destabilizes symbiotic nutrient cycling in corals. *Proc.*
832 *Natl. Acad. Sci.* **118**, e2022653118 (2021)
833 24. Vega Thurber, R. et al. Deciphering Coral Disease Dynamics: Integrating Host,
834 Microbiome, and the Changing Environment. *Front. Ecol. Evol.* **8**, 575927 (2020)
835 25. Dimond, J. L. & Roberts, S. B. Convergence of DNA Methylation Profiles of the
836 Reef Coral *Porites astreoides* in a Novel Environment. *Front. Mar. Sci.* **6**, 792 (2020)
837 26. Dixon, G., Liao, Y., Bay, L. K. & Matz, M. V. Role of gene body methylation in
838 acclimatization and adaptation in a basal metazoan. *Proc. Natl. Acad. Sci.* **115**,
839 13342–13346 (2018)
840 27. Dixon, G. B., Bay, L. K. & Matz, M. V. Bimodal signatures of germline methylation
841 are linked with gene expression plasticity in the coral *Acropora millepora*. *BMC*
842 *Genomics* **15**, 1109 (2014)

843 28. Putnam, H. M., Davidson, J. M. & Gates, R. D. Ocean acidification influences host
844 DNA methylation and phenotypic plasticity in environmentally susceptible corals.
845 *Evol. Appl.* **9**, 1165–1178 (2016)
846 29. Liew, Y. J. et al. Intergenerational epigenetic inheritance in reef-building corals. *Nat.*
847 *Clim. Change* **10**, 254–259 (2020)
848 30. Rodríguez-Casariego, J. A. et al. Coral epigenetic responses to nutrient stress:
849 Histone H2A.X phosphorylation dynamics and DNA methylation in the staghorn
850 coral *Acropora cervicornis*. *Ecol. Evol.* **8**, 12193–12207 (2018)
851 31. Guerrero, L. & Bay, R. Patterns of methylation and transcriptional plasticity during
852 thermal acclimation in a reef-building coral. *Evol*. *Appl*. **17**, e13757 (2024)
853 32. Abbott, E., Loockerman, C., & Matz, M. V. Modifications to gene body methylation
854 do not alter gene expression plasticity in a reef-building coral. *Evol*. *Appl*. **17**, e13662
855 (2024)
856 33. Rodríguez-Casariego, J. A. et al. Genome-Wide DNA Methylation Analysis Reveals
857 a Conserved Epigenetic Response to Seasonal Environmental Variation in the
858 Staghorn Coral *Acropora cervicornis*. *Front. Mar. Sci.* **7**, 560424 (2020)
859 34. Turgut-Kara, N., Arikan, B. & Celik, H. Epigenetic memory and priming in plants.
860 *Genetica* **148**, 47–54 (2020)
861 35. Konciute, M. K. Exploring the Role of Glutamate Signaling in the Regulation of the
862 *Aiptasia*-Symbiodiniaceae Symbiosis. *KAUST Research Repository* (2020)
863 36. Kawamura, K. et al. *In vitro* Symbiosis of Reef-Building Coral Cells With
864 Photosynthetic Dinoflagellates. *Front. Mar. Sci.* **8**, 706308 (2021)
865 37. Kamran, Z. et al. In vivo imaging of epithelial wound healing in the cnidarian *Clytia*
866 *hemisphaerica* demonstrates early evolution of purse string and cell crawling closure
867 mechanisms. *BMC Dev. Biol.* **17**, 17 (2017)
868 38. Agarwal, S. et al. Autophagy and endosomal trafficking inhibition by *Vibrio cholerae*
869 MARTX toxin phosphatidylinositol-3-phosphate-specific phospholipase A1 activity.
870 *Nat. Commun.* **6**, 8745 (2015)
871 39. Kimes, N. E. et al. Temperature regulation of virulence factors in the pathogen *Vibrio*
872 *coralliilyticus*. *ISME J.* **6**, 835–846 (2012)

873 40. Dixon, G. & Matz, M. V. Changes in gene body methylation do not correlate with
874 changes in gene expression in Anthozoa or Hexapoda. *BMC Genomics* **23**, 234 (2022)
875 41. Lehnert, E. M., Mouchka, M. E., Burriesci, M. S., Gallo, N. D., Schwarz, J. A., &
876 Pringle, J. R. Extensive Differences in Gene Expression Between Symbiotic and
877 Aposymbiotic Cnidarians. *G3 Genes|Genomes|Genetics* **4**, 277-295 (2014)
878 42. Pacherres, C. O., Ahmerkamp, S., Koren, K., Richter, C., & Holtappels, M. Ciliary
879 flows in corals ventilate target areas of high photosynthetic oxygen production. *Curr*.
880 *Biol*. **32**, 4150-4158 (2022)
881 43. Hansen, S. B. et al. Intestinal epigenotype of Atlantic salmon (*Salmo salar*) associates
882 with tenacibaculosis and gut microbiota composition. *Genomics* **115**, 110629 (2023)
883 44. Garcias-Bonet, N. et al. Horizon scanning the application of probiotics for wildlife.
884 *Trends Microbiol.* S0966-842X(23)00259-7 (2023)
885 45. Peixoto, R. S., Sweet, M. & Bourne, D. G. Customized Medicine for Corals. *Front.*
886 *Mar. Sci.* **6**, 686 (2019)
887 46. Peixoto, R. S. & Voolstra, C. R. The baseline is already shifted: marine microbiome
888 restoration and rehabilitation as essential tools to mitigate ecosystem decline. *Front.*
889 *Mar. Sci.* **10**, 1218531 (2023)
890 47. Voolstra, C. R. & Ziegler, M. Adapting with microbial help: microbiome flexibility
891 facilitates rapid responses to environmental change. *BioEssays*. **42**, 7 (2020)
892 48. Dixon, G. & Matz, M. Benchmarking DNA methylation assays in a reef-building
893 coral. *Mol. Ecol. Resour.* **21**, 464-477 (2021)
894 49. Wilcoxon, F. Individual Comparisons by Ranking Methods. *Biometrics Bulletin* **1**,
895 80-83 (1945)
896 50. Kruskal, W. H. & Wallis, W. A. Use of ranks in one-criterion variance analysis. *J.*
897 *Am. Stat. Assoc.* **47**, 583–621 (1952)
898 51. Dunn, O. J. Multiple Comparisons Using Rank Sums. *Technometrics* **6**, 241–252
899 (1964)
900 52. Martin, M. Cutadapt removes adapter sequences from high-throughput sequencing
901 reads. *EMBnet.journal* **17**, 10–12 (2011)
902 53. Callahan, B. J. et al. DADA2: High-resolution sample inference from Illumina
903 amplicon data. *Nat. Methods* **13**, 581–583 (2016)

904 54. Quast, C. et al. The SILVA ribosomal RNA gene database project: improved data
905 processing and web-based tools. *Nucleic Acids Res.* **41**, D590–D596 (2013)
906 55. McMurdie, P. J. & Holmes, S. phyloseq: An R Package for Reproducible Interactive
907 Analysis and Graphics of Microbiome Census Data. *PLoS ONE* **8**, e61217 (2013)
908 56. Altschul, S. F., Gish, W., Miller, W., Myers, E. W. & Lipman, D. J. Basic Local
909 Alignment Search Tool. *J Mol Biol* **215**, 403–410 (1990)
910 57. Buitrago-López, C., Mariappan, K. G., Cárdenas, A., Gegner, H. M. & Voolstra, C.
911 R. The Genome of the Cauliflower Coral *Pocillopora verrucosa*. *Genome Biol. Evol.*
912 **12**, 1911–1917 (2020)
913 58. Krueger, F. & Andrews, S. R. Bismark: a flexible aligner and methylation caller for
914 Bisulfite-Seq applications. *Bioinformatics* **27**, 1571–1572 (2011)
915 59. Alexa, A., Rahnenführer, J. & Lengauer, T. Improved scoring of functional groups
916 from gene expression data by decorrelating GO graph structure. *Bioinformatics* **22**,
917 1600–1607 (2006)
918 60. Bray, N. L., Pimentel, H., Melsted, P. & Pachter, L. Near-optimal probabilistic RNA-
919 seq quantification. *Nat. Biotechnol.* **34**, 525-527 (2016)
920 61. Pimentel, H. J., Bray, N., Puente, S., Melsted, P. & Pachter, L. Differential analysis of
921 RNA-seq incorporating quantification uncertainty. *Nat. Methods* **14**, 687-690 (2017)